Comparative study of vibration measuring techniques applied to Aluminum beams with localized damage

Edson Vinícius Garcia da Silva

A dissertation presented to

Escola Superior de Tecnologia e Gestão

Instituto Politécnico de Bragança

In partial fulfillment of the requirements for the degree of

Master of Industrial Engineering

February 2019

Comparative study of vibration measuring techniques applied to Aluminum beams with localized damage

Edson Vinícius Garcia da Silva

A dissertation presented to

Escola Superior de Tecnologia e Gestão

Instituto Politécnico de Bragança

In partial fulfillment of the requirements for the degree of

Master of Industrial Engineering

In double degree program with

Universidade Tecnológica Federal do Paraná

Supervisors: Prof. Dr. João Ribeiro

Prof. Dr. Giovanni Bratti

Prof. Dr. Manuel Braz César

February 2019

ACKNOWLEDGEMENTS

This section has the purpose to say thank you to the important people who helped me along my academic life. Since most of them do not speak English, there is no reason to write this part in English. The following text is in Portuguese.

Dedico este trabalho aos meus pais, que sempre se esforçaram ao máximo para que eu pudesse chegar neste momento tão importante. Foram muitos anos me apoiando e me incentivando a ser sempre melhor, a me dedicar e a não desistir. Obrigado!

Gostaria de agradecer aos meus orientadores, professor João Ribeiro, professor Giovanni Bratti e professor Braz César, por todo o apoio que recebi durante a elaboração deste trabalho, bem como ao IPB e à UTFPR pela oportunidade de viver uma experiência única.

Também devo agradecimento a algumas pessoas que foram essenciais durante toda minha vida acadêmica, sem as quais talvez eu não chegaria neste momento:

À minha família pelo apoio incondicional ao longo de todos esses anos. Em especial aos meus avós, que sempre foram exemplo de caráter e resiliência sem deixar de ser um porto seguro e fonte de aconchego nas horas de necessidade.

Aos meus irmãos que, mesmo longe, foram uma fonte de motivação para que eu sempre tenha seguido em frente.

Aos meus tios, por todo o apoio prestado, pelos conselhos profissionais e por todo o companheirismo ao longo de todos esses anos.

Às minhas primas, por sempre alegrarem minha vida, pelo companheirismo e por sempre me apoiarem.

Aos meus amigos, Erick Sutil, Bruno Fortes, Lucas Dobkowski, Sharlane, Queli Freitas e Gustavo por fazer minha vida muito melhor e mais alegre durante todos esses anos e, também, por estarem sempre ao meu lado nos bons e maus momentos. À Eloisa, por ter se dedicado a mim por tanto tempo e por estar ao meu lado durante tantos anos, nas mais diversas situações.

Aos meus amigos feitos em Bragança: Francieli, Maiz, Heloisa e Bernardo por tornar essa experiência melhor do que jamais imaginei, pelos momentos inesquecíveis e pelos aprendizados ao longo do caminho. À Nadine, por todo o apoio prestado, sempre com um sorriso no rosto e positividade.

À Spec-man, por todo o apoio fornecido para que o trabalho pudesse ser realizado.

ABSTRACT

When a structural damage changes the characteristics of stiffness and mass of a mechanical system, the dynamic behavior of this beam will also change. Only a few studies about the correlation between damage and the effect caused in dynamic behavior can be found. Based on this, this study will analyze the behavior of the natural frequencies and damping ratios of four aluminum beams, with and without damages.

This work aims to determine the error between the two methods of data acquisition and the effects of the damage inflicted on the shape modes, natural frequencies and damping ratios for each beam.

To achieve the purposes, initially, a numerical FEM simulation will be performed, followed by experimental impact tests, aiming to obtain the estimated natural frequencies and damping ratios. After this, damages will be made on these beams and the impact tests will be repeated for each beam.

The FEM analysis will be performed using Ansys. For the impact tests, two data acquirement methods will be used during the impact testing, the first, using accelerometers to obtain the vibration response, the second using a Brüel & Kjær's sound level meter. The obtained data will be compared and will be possible to determinate the error between the natural frequencies measured using both methods. The results obtained will be used to correlates the dynamic behavior with the damages inflicted on the beams.

This paper allowed analyzing the usage viability of the sound level meter to measure the output of a vibrating system, considering certain limitations. In addition, the damage effects on the natural frequencies of the beams.

RESUMO

Quando um dano altera as características de massa e rigidez de um sistema (uma viga, por exemplo), seu comportamento dinâmico também é afetado. O estudo dos efeitos do dano infligido no comportamento modal é relativamente recente, tendo poucos estudos correlacionando o dano com seus efeitos em vigas. Baseado nisso, este estudo visa analisar o comportamento e variação do valor das frequências naturais e dos fatores de amortecimento de quatro vigas de alumínio com e sem danos.

Este trabalho tem por objetivo determinar: o erro entre as medições efetuadas utilizando ambos os métodos de obtenção da resposta de vibração das vigas e os efeitos dos danos causados no comportamento modal do sistema analisado (modos de vibração, frequências naturais e fatores de amortecimento).

Para tal, incialmente, uma simulação numérica utilizando elementos finitos será efetuada, seguida por testes de impacto, com o objetivo de obter as frequências naturais e os fatores de amortecimento para cada caso.

A simulação numérica será efetuada utilizando o *software* Ansys e os testes de impacto utilizarão dois métodos de aquisição da resposta do sistema: utilizando acelerômetros e um medidor de pressão sonora. Os dados obtidos serão comparados e será possível determinar o erro entre os métodos de medição utilizados. Os resultados obtidos também serão utilizados para analisar os efeitos dos danos no comportamento dinâmico das vigas utilizadas.

A elaboração deste trabalho possibilitou averiguar a viabilidade do uso de um medidor de pressão sonora para medição de vibrações, dentro de seus limites de utilização e suas limitações. Também foi possível analisar os efeitos dos danos nos valores de frequências naturais das vigas analisadas.

SUMMARY

1. INTRODUCTION 1

1.1. Background 1

1.2. Main goals and work organization 2

2. THEORY SECTION 5

2.1. Vibrations 5

2.2. Modal analysis 6

2.2.1. Modal testing or Experimental Modal Analysis (EMA) 6

2.2.2. Hysteretically damped multiple degree of freedom systems 12

2.2.3. Frequency response functions 15

2.3. Sound and Vibration 17

2.3.1. Definition and measurement parameters 17

2.3.2. Sound radiation in plates 18

2.3.3. Correlation with vibrations 19

2.4. Damage and its effects 19

2.5. Structure Health Monitoring 20

2.6. Model updating 22

3. MATERIALS AND METHOD 23

3.1. Materials and geometries 23

3.2. Methods 25

3.2.1. Numerical method 25

3.2.2. Experimental method 25

4. RESULTS AND ANALYSIS 33

4.1. Beam number 1 33

4.1.1. Natural frequencies 33

4.1.2. Mode shapes 35

4.1.3. Damping ratios 37

4.2. Beam number 2 38

4.2.1. Natural frequencies 38

4.2.2. Mode shapes 41
4.2.3. Damping ratios 42
4.3. Beam number 3 43
4.3.1. Natural frequencies 43
4.3.2. Mode shapes 46
4.3.3. Damping ratios 48
4.4. Beam number 4 49
4.4.1. Natural frequencies 49
4.4.2. Mode shapes 52
4.4.3. Damping ratios 54
4.5. Impact tests to determine the torsional natural frequency 54
4.6. Global results 56
4.7. Natural frequency 57
4.8. Damping ratios 59
4.9. FRF analysis 60
5. DISCUSSION 63
5.1. Natural frequencies 63
5.1.1. Damage effects 63
5.1.2. Tests using accelerometer and the sound level meter 64
5.2. Mode shapes 65
5.3. Damping ratios 66
5.4. Frequency response functions 66
6. CONCLUSIONS AND FUTURE RESEARCH SUGGESTIONS 69
6.1. Conclusions 69
6.2. Future research suggestions 70
LIST OF REFERENCES 71
APPENDIX A 75
APPENDIX B 77

TABLE INDEX

Table 1. Definition of Frequency Response Functions [9], modified. 16
Table 2. Perforation dimensions used. 23
Table 3. Impact of the damage on the mass and moment of inertia of the analyzed beams. 24
Table 4. Errors between the measured values using the accelerometer and the sound level meter for Beam number one. 34
Table 5. Errors between the measured values using the accelerometer and the sound level meter for Beam number two. 41
Table 6. Errors between the measured values using the accelerometer and the sound level meter for Beam number three. 46
Table 7. Errors between the measured values using the accelerometer and the sound level meter for Beam number four. 52
Table 8. Values estimated and measured for ω_{n3}. 56
Table 9. Properties of the beams. 75
Table 10. Errors between the estimated and measured (using accelerometer) natural frequencies. 78
Table 11. Errors between the estimated and measured (using the sound level meter and accelerometer) natural frequencies. 79
Table 12. Errors between the estimated and measured (using the sound level meter) natural frequencies. 80
Table 13. Errors between the measured natural frequencies (accelerometer and sound level meter). 81
Table 14. Errors between the measured natural frequencies (accelerometer and sound level meter with the accelerometer). 82

FIGURE INDEX

Figure 1. Work organization steps. 4
Figure 2. Theoretical (a) and experimental (b) routes to vibration analysis. 8
Figure 3. Schematic representation of an EMA. 15
Figure 4. Characteristic energy flux irradiated by a rectangular plate in resonance [24]..... 18
Figure 5. Excitation and output points..... 26
Figure 6. Impact test using an accelerometer as an output source. 28
Figure 7. Impact test using a sound level meter as an output source. 30
Figure 8. Estimated and measured frequencies for beam number one. 35
Figure 9. Mode shapes obtained for the beam number one. 36
Figure 10. Damping ratios measured for beam number one. 37
Figure 11. Estimated and measured frequencies for beam number two. 40
Figure 12. Mode shapes obtained for the beam number two. 42
Figure 13. Damping ratios measured for beam number two. 43
Figure 14. Estimated and measured frequencies for beam number three. 45
Figure 15. Mode shapes obtained for the beam number three. 47
Figure 16. Sixth mode shape to $T_{3,2}$ and $T_{3,3}$. 48
Figure 17. Damping ratios measured for beam number three..... 49
Figure 18. Estimated and measured frequencies for beam number four. 51
Figure 19. Mode shapes obtained for the beam number four (test one to six).... 53
Figure 20. Fourth and fifth mode shapes for test number seven on beam number four. 53
Figure 21. Damping ratios measured for beam number four. 54
Figure 22. Global analysis of the first natural frequency variation along the tests. 57
Figure 23. Global analysis of the second natural frequency variation along the tests. 58
Figure 24. Global analysis of the third natural frequency variation along the tests. 58
Figure 25. Global analysis of the fourth natural frequency variation along the tests. 59

Figure 26. Damping ratios measured along the tests. 60
Figure 27. FRFs for the selected tests performed. 61
Figure 28. Schematic of the damaged beam. Dimensions in mm. 75
Figure 29. Sixth mode shape for $T_{4,7}$ (1650,7 Hz). 77

LIST OF ABREVIATIONS

DOF – Degree Of Freedom

DR – Damping Ratio

EMA – Experimental Modal Analysis

FEM – Finite Element Method

FFT – Fast Fourier Transform

FRF – Frequency Response Function

MDOF – Multiple Degree Of Freedom

MIMO – Multi-Input Multi-Output

NA – Not Applicable

ODS – Operating Deflection Shape

OMA – Operational Modal Analysis

SHM – Structural Health Monitoring

SIL – Sound Intensity Level

SIMO – Single-Input Multi-Output

SISO – Single-Input Single-Output

1. INTRODUCTION

1.1. Background

Mechanical structures are designed to support repetitive and static loadings, friction and temperature and pressure variations. The combination of all this efforts cause structural deterioration and can lead the mechanism to an unexpected failure. An efficient and precise method to detect and evaluate the damage caused by the deterioration can be crucial to prevent the failures and to provide an effective path to reduce the maintenance cost. The importance of reducing failure of the mechanical systems and the maintenance costs led to the development of techniques used to detect and oversee the structural damage, allowing to keep track of the damages and its effects [1], [2].

A repetitive loading found in most mechanical structures is the system's vibration that can cause failure by material fatigue, because of the cyclic variation of the stress induced to the system. Furthermore, a vibrational problem can cause faster wear of system's components, such as bearings and gears. Also it can create excessive noise levels that can be prejudicial to human health, for example [1]. That is why vibration level and damages must be frequently monitored. One method used to monitor the vibrational effects is the Structural Health Monitoring (SHM). SHM is a Non-Destructive Evaluation method that aims to give a diagnosis of the working condition and of the constituting material conditions of the many parts that compose the structure and the completely mechanical system. Its temporal dimension also allows to obtain a prognosis of the system, so it is possible to evaluate the evolution of the damage and to predict a residual life to it [3].

Every system has a set of vibration characteristics, being they, the natural frequencies, the mode shapes and the damping of the system. These modal characteristics are affected by the system's physical characteristics, more specifically the stiffness and mass. A damage usually causes changes to the system's stiffness and/or mass, affecting, directly, the vibration characteristics of the system. Therefore, theoretically, it is possible to detect, monitor and determine the severity of a damage caused to a mechanical system by measuring its vibration characteristics. Vibration-based techniques to monitor the structural health offers several vantages: the damage location does not need to be known; the sensors required to measure the vibration

characteristics does not need to be too close to the damaged area; and a limited number of sensors can, usually, provide enough information to locate and determine the severity of a damage, even in a large and complex structure [4], [5]. However, in practice, the vibration-based assessment has a number of limitations, like the low sensitivity that a global system has to a local damage, the incomplete nature of the measured vibration characteristics and other factor's (such as thermal loading) influence in the data acquired [4].

Usually, modal data is acquired using piezoelectric sensors on the system under analysis but it is not the only way to obtain the necessary information to the modal analysis.

When an object vibrates on an elastic fluid ambient (air, for example), its vibration induces pressure oscillations on the medium. These pressure oscillations can be measured using a microphone. Using the assumption that, at a particular frequency, the sound pressure levels emitted by a vibrating structure vary linearly with vibration amplitudes allows to consider that the modal coefficient of the input point is directly proportional to the sound level. Since the modal coefficient is proportional to the amplitude of the structure's response at each natural frequency, some modal data (such as natural frequencies and damping factor) can be estimated using the data measured with the microphone. The procedure described is known as an acoustic approach to obtain the modal data and it is most used in cases where accelerometers usage is limited by mounting issues or on structures where the accelerometer's mass can affect its dynamic behavior [6], [7].

1.2. Main goals and work organization

The main goal of this work is to analyze and compare two methods of data acquisition to obtain the dynamic response of the mechanical system: using accelerometers (usually piezoelectric accelerometers) and using a sound level meter. Yet there are two secondary goals: detect the damage inflicted to the system under analysis and, if possible, determine its location.

Four aluminum beams compose the system under analysis. Initially the beams have no damage.

The work organization will follow the steps bellow:

1. Modal analysis using a Finite Element Method (FEM): each beam will be modeled using a FEM method and then a modal analysis will be performed, individually, using the Ansys software. The main goal is to obtain a set of reference modal parameters (natural frequency and mode shapes).

2. Impact test to obtain the natural frequencies and damping ratio: two impact tests will be performed on each beam: at first, using a piezoelectric sensor (accelerometer), after using a sound level meter to obtain the response data (displacement and acoustic response, respectively). The main goal is to measure the natural frequencies and damping ratios of the undamaged systems.

3. Damage infliction: the beams will be perforated, damaging the mechanical system.

4. Impact test to obtain the natural frequencies and damping ratio: the damaged systems will be submitted, again, to two impact tests, using the same method of the undamaged system. The main goal is to measure the natural frequencies and damping ratios of the damaged condition.

5. Data analysis and comparison: having both modal parameters (undamaged and damaged case scenarios) allows to analyze and compare the measured data, aiming to determine the difference between the two methods and if the sound level meter is reliable when used to obtain the natural frequencies and damping ratio of a mechanical system. Moreover, if possible, the damage detection and if its location can be determined in this scenario.

A more intuitive vision of all these steps is available in the Figure 1 bellow:

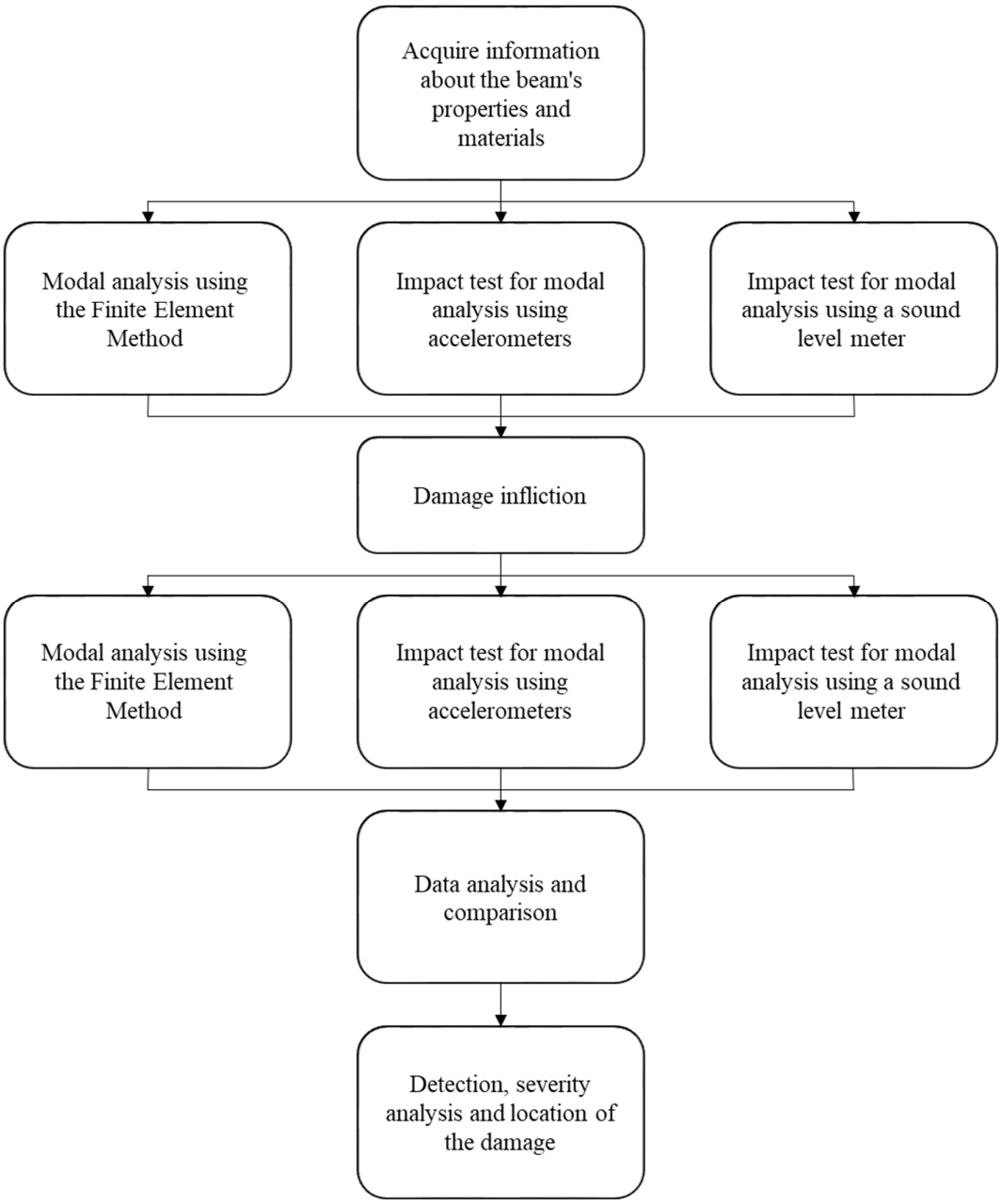

Figure 1. Work organization steps.

2. THEORY SECTION

This chapter contains the main theoretical concepts necessary to understand the theory used in this work.

At first will be presented an introduction to mechanical vibrations, its importance and the main concepts. After, the modal analysis will be approached, describing the processes, components and methods currently in use. Subsequently, the acoustic approach and its correlations with vibrations. Finally, at last, the damage and its effects in mechanical structures in vibration condition.

2.1. Vibrations

Inman [8] defines vibrations as “the study of the repetitive motion of objects relative to a stationary frame of reference or nominal position (usually equilibrium)”. A vibrational system must have potential energy, kinetic energy and a mass. The mass must release the potential energy as kinetic energy (in the form of motion) and restore the kinetical energy as potential energy, alternately [8].

Vibration is present in many human activities, one way or another. For example, we hear because our eardrums vibrate when excited by an external source of vibration, this external source may be someone speaking (it is possible because the vocal cords have an oscillatory movement), creating a sound wave that vibrates de air and reaches our ears [1]. Music also involves vibration, a guitar, for example, produces sound due to the string vibration that reaches our ears allowing us to listen the music [8].

Vibration can be desirable, like when we speak, or not desirable, like in most of the mechanical systems and structures. Vibration can cause fatigue and lead the structure to a non-programed failure or cause excessive noise problems.

The resonance phenomenon happens when the structure vibrates on its natural frequency. This phenomenon is, usually, undesired and causes excessive deflections of the system [1], [8].

A vibrational system is classified according to its vibrating condition (free or forced vibration), according to its damping conditions (damped and undamped systems) or according to the equations that describes its motion (linear or nonlinear systems) [1].

It is worth remembering that the superposition principle is valid only to linear vibrational systems.

2.2. Modal analysis

The system durability is of great concern during the design phase, being important to consider its dynamic behavior. If the vibration levels exceed the elastic limits of the system, this can cause several damage and catastrophic failure to the system.

Systems are projected using ideal concepts (the material is homogeneous and isotropic; the stiffness is constant, etc.). However, the properties of real materials can be slightly different from the theoretical ones. Examples of it are materials with some pores in or orthotropic characteristics due to the manufacturing processes.

Because there are differences between the system's theoretical and real model, an experimental study is necessary to characterize the real dynamic behavior of the system. One way to do this is through the modal analysis, described below.

2.2.1. Modal testing or Experimental Modal Analysis (EMA)

Ewins [9] defines modal testing as "the processes involved in testing components or structures with the objective of obtaining a mathematical description of their dynamic or vibration behavior". In other words, the modal testing is the procedure used to identify the modal parameters (natural frequencies, damping factors and modal shapes) of a real structure, when subjected to external excitations.

Although the modal testing has a great importance when studying the dynamic behavior of some structure or system, the theory is relatively new. One of the more important studies dates back from 1947 with the Kennedy and Pancu [10]. Along the years, more frequently to the aero spacing projects, the methods evolved. The technology advances in the computational, transducers and electronics fields allowed this method to be more accurate [9].

Perhaps the most used application of modal testing is to measure the system's vibration properties, allowing comparing the measured data and the one used during the theoretical project. After the data is acquired and analyzed it becomes possible to update the numerical model and new simulations can be performed (this procedure is known as "model updating" and will be discussed below) [9], [11].

Experimental modal analysis is an extremely important method to validate the theoretical models, to identify vibrations of a structure and to detect structural

modifications [12]. By the 1970's, the use of EMA was facilitated by the development of the digital analyzers. Today, devices like impact hammer allow the tests to be fast and economic to characterize a structure [13].

2.2.1.1. Basic measurement chain and necessary equipment

The basic route to a vibration analysis may be split in two parts. The first is the theoretical part, which involves the spatial model, the modal model and the response model. The spatial model describes the structure in terms of mass, stiffness and damping. The modal model describes the structure's behavior as a set of natural frequencies with corresponding modal damping factors and vibration mode shapes. The response model describes the frequency and impulse responses, i.e., how the structure will respond when an excitation is applied to it, it is composed by a set of frequency response functions (FRFs) [9].

In the other hand, the experimental part happens the other way. When a structure is tested using modal analysis, the obtained response properties, with the calculated modal properties, can be used to deduce a structural model for the structure. The hypothesis used to estimate the modal properties could be improved and used to get better accuracy results by updating the structural model every time a new analysis is performed [9].

Figure 2 displays a visual description of the theoretical and the experimental route to perform a vibration analysis.

In order to ensure a high quality of the acquired data there are some aspects to consider when planning the measurement process, they are [9]:

1. The mechanical aspect of supporting and exciting the structure;
2. The correct transduction of the data to be measured (force input and motion response); and
3. The signal processing must be appropriated to the type of test used.

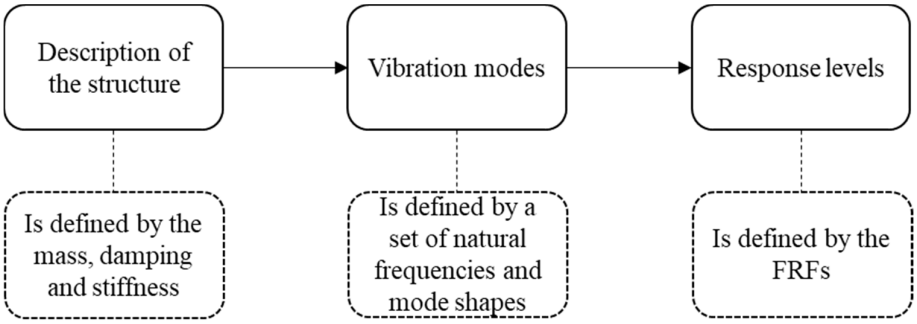

(a). Route of a theoretical vibration analysis.

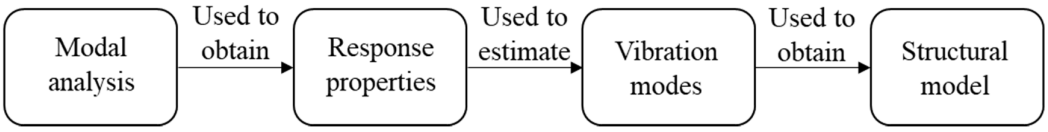

(b). Route of an experimental vibration analysis.

Figure 2. Theoretical (a) and experimental (b) routes to vibration analysis.

The first aspect to be observed is how the structure will be supported (it can be suspended or supported) and how the initial condition (usually a displacement caused by an applied force) will be applied [9], [11]. There are some options of support to be considered, first the "Free" (or "Unrestrained") support is a term used when the structure to be analyzed is suspended using very soft springs (like rubber chords, for example) or laying down on a soft surface (a foam pad, for example). There is also the "Grounded" support, which implies that the test structure is hold to a fix support, usually clamping the test object to a larger structure (representing a rigid connection). Finally, the "In situ" condition of support, this condition is used when the test object is connected with some other structure or component but the attachment is a non-rigid connection [9].

The exciting method, the second and third aspects depends directly on the availability and quality of the equipment available to use. Also, three main measurement mechanisms require a special attention [11]:

i. The excitation mechanism;
ii. The sensing mechanism; and
iii. The data acquisition and processing mechanism.

The excitation mechanism is the one that provides the initial condition to the system. Usually the initial condition is a motion applied to the structure by a force (*f(t)*) applied to a previously determined position.

There are some devices available to apply the initial condition and the choice depends on factors such as: the desired input (a single impact or a repeating force), accessibility and the physical properties of the structure [11].

Shakers (or exciters) are electromagnetic or hydraulic vibrators, driven by a controller device, which controls the frequency and/or amplitude of the force applied to the structure to match the input requirements of the structure under test. Due to the high controllability of the shakers, they can be considered the most accurate input condition option. Using a shaker also provides the possibility of analyzing a specific range of frequencies. However there are some disadvantages of using a shaker, one of them is the need to have a connection between the shaker and the test structure (usually a force transducer is used), causing attachment influence which influence the measured response, which is always undesirable [1], [11].

An alternative to the shaker is the impact hammer (also known as an impulse hammer). It is a simple hammer, usually with a controllable amount of mass, equipped with a force transducer (usually a piezoelectric sensor) on its tip (the force transducer makes possible to know the applied force during the impact). The impact method dismisses the need to have a signal generator and a power amplifier. The hammer excites a large range of frequencies, making harder to analyze a specific behavior on a specific frequency. Another issue when performing an impact test is to provide a single impact to the structure, sometimes a second impact takes place after the first and, generally, the test has to be performed again. Yet it is hard to control the applied force direction when using the hammer. However, the hammer does not require an attachment to the system, reducing the attachment influence also the impact test is faster than the one that uses the shaker. The frequency range covered by the hammer depends on the hammer mass, the hammer tip and the impact velocity, which dictate the amplitude of the force applied to the test structure [1], [11].

Devices, known as transducers, constitute the sensing mechanism. The most popular transducers are the piezoelectric. A piezoelectric transducer is designed to produce electric signals proportional to either force (force transducers) or acceleration (accelerometers) applied on the piezoelectric cell. Most of the time the signal generated for the piezoelectric cell is very weak to be directly measured and processed but the

problem can be easily solved by using a signal amplifier [1], [11]. Just like the shaker, the transducers need to be connected to the structure, so it also generates attachment influence.

Finally, the data acquisition and processing system (or mechanism), is the one responsible for measure the signal developed by the sensing mechanism. After a signal conditioner amplifies the signal, the electric signal needs to be digitized so it is possible to process and analyze the signal on a computer. A very common type of analyzer is the Fast Fourier Transform[1] (FFT) analyzer. The FFT analyzer receives an analogue voltage signal (representing the measured item, such as force, acceleration or displacement), filter it and digitize for further analysis [1], [11].

The analysis can be performed using a single input or multiple inputs (the same is valid to the output). When using a single input and a single output sensor the test is known as "single-input single-output" (SISO). A SISO test implies that the input signal comes from one only transducer and the output signal, also, comes from only one transducer. The SISO technique has the advantage of requiring less equipment (it is cheaper) and, usually, does not cause a mass overload on the system because there is only one accelerometer attached to the structure under test. However, it has the disadvantage of measuring limited data so, if the system is complex and require a large amount of data, several tests will have to be performed in order to obtain the necessary amount of data.

An alternative to the SISO technique is the multi-input multi-output (MIMO) technique. This technique uses multiple excitations sources and multiple output transducers. Although it is more expensive than the SISO technique, the multiple-output transducers allow a larger data collection on a single test, and, the multiple-input sources allow better energy distribution over the structure. Usually, MIMO tests are used when the structure under analysis is large or complex [14], [15].

Alternatively, there is the single-input multi-output (SIMO) technique. This technique allows a larger data measurement, when compared with the SISO technique, and requires only one excitation source [14], [15].

[1] FFT is a mathematical expression that converts a signal from its original domain (usually time domain) to the frequency domain.

2.2.1.2. Operational Modal Analysis

When a structure is in operation, most of the times, it is not possible to define, exactly, all the forces acting on it. The unknown forces acting on the structure may be insignificant to the dynamic behavior but, sometimes, these forces can be the ones that lead the structure to fail.

The Operational Modal Analysis (OMA - also called "output-only modal analysis") is an alternative method to obtain the dynamic properties of the structure simple by measuring the response of the structure, i.e., OMA does not use an artificial excitation, dismissing the excitation mechanism [16].

There are some advantages when comparing the operational and the traditional experimental modal analysis. OMA is performed while the structure is under operation. That means the loads acting in the structure and the boundary conditions are real and there is no need to approximate them. Another advantage of using OMA instead of EMA is the possibility of performing the analysis in-situ, i.e., there is no need to remove a part of the structure to be tested, also these test does not need to interrupt the daily activities of the structure [16].

2.2.1.3. Operating Deflection Shapes

Ewins [9] refers to operating deflection shape (ODS) as "the resulting vector of responses" of a structure when it has received some excitation. The quote above makes an ODS sound just like a mode shape but they are quite different. Mode shapes are inherent properties of a structure, i.e., they depend on mass, stiffness, damping of the structure and the boundary conditions but they are not affected for changes of forces or loading acting on the structure, also, a mode shape has not a dimension associated to it. Though an ODS depends on the forces and loads applied to the structure and they will change if the load changes and an ODS has a dimension associated (for instance, displacement, velocity or acceleration units). Finally, modes are only used to characterize resonant vibrations while ODS can be defined for non-resonant vibration responses [17].

An alternative definition to ODS is used by Schwarz and Richardson [17], [18], the refer to and ODS as "any forced motion of two or more points". While a mode shape is a specific mode associated to a natural frequency the ODS represents how

much the structure moves, when excited, at a particular time or frequency [17]. Yet, when the excitation frequency is close to some structure's resonant frequency the ODS will, usually, reflect the mode shape associated to it, but will not be identical because there are other mode shapes contributing to the vibration [9].

Finding the ODS helps to answer how much the structure is vibrating, where are located the critical points of its dynamic response, if the frequency excited is a resonant one, which shape it looks like and contribute to determine correct actions to reduce the vibration level [18].

However, there is a factor that difficult to perform an ODS analysis. As mentioned before, the ODS depends on the motion of two or more points so, if the operation is not repeatable, a multi-channel acquisition system must be used, what require an additional number of transducers (they may cause mass influence) and more sophisticated signal conditioning equipment. If the operation is repeatable the ODS data can be acquired using only one transducer and a single channel analyzer but must be performed, at least, twice (one for each point of interest). To be repeatable, the operation must allow that the data acquisition occur when the exactly same time waveform is obtained in the sampling window [18].

2.2.2. Hysteretically damped multiple degree of freedom systems

Rao [1], defines the term "degree(s) of freedom" (DOF) as "the minimum number of independent coordinates required to determine completely the positions of all parts of a system at any instant of time". A multiple degree of freedom system (MDOF) is a system that has more than one DOF.

A common vibrating system has infinite DOFs implying it must be discretized to allow obtaining an approximated solution. The discretization process divides the continuous system in smaller parts represented by a new lumped-mass system. The system must be divided as many times as necessary to ensure the accuracy of the solution [11].

For a hysteretically damped MDOF system, the equation that rules its vibrations has the form:

$$[M]\{\ddot{x}(t)\} + i[D]\{x(t)\} + [K]\{x(t)\} = \{f(t)\} \quad (1)$$

where [M], [D] and [K] are n x n mass, hysteretic damping and stiffness symmetric matrices, respectively, describing the spatial properties of the system. N is the system's DOF number. The column vectors $\{\ddot{x}(t)\}$ and $\{x(t)\}$ are Nx1 time-dependent acceleration and displacement response vectors, respectively. $\{f(t)\}$ is an Nx1 time-dependent external excitation vector [11].

Equation (1) represents the N second order differential equations that must be solved simultaneously in order to obtain the required information about the system [11].

Assuming that the damping is proportional to the stiffness and mass of the system we can describe the [D] matrix as:

$$[D] = \varepsilon[K] + \nu[M] \tag{2}$$

where ε and ν are constants. Assuming that a solution exists and has the form:

$$\{x(t)\} = \{\bar{X}\}e^{i\lambda t} \tag{3}$$

where $\{\bar{X}\}$ is an Nx1 response amplitude vector and it's time-independent. Substituting Equation (3) into the homogeneous form of Equation (1), we obtain [11]:

$$\big([K] - \lambda^2[M] + i(\varepsilon[K] + \nu[M])\big)\{\bar{X}\} = \{0\} \tag{4}$$

Equation (4) represents a complex eigenvalue problem and leads to a solution in terms of n complex eigenvalues λ_r^2 and N real eigenvectors $\{\Psi_r\}$. The eigenvectors $\{\Psi_r\}$ are the same obtained in the undamped case (obtained solving the system described in Equation (4)) and have the same physical meaning, i.e., they describe the same mode shapes [11].

Taking λ_r^2 as containing information on the natural frequencies of the system, we can write:

$$\lambda_r^2 = \omega_r^2(1 + i\,\eta_r) \tag{5}$$

Where ω_r^2 and η_r are the natural frequency and damping loss factor, respectively. For mode *r*, the natural frequency is defined as:

$$\omega_r^2 = \frac{k_r}{m_r} \tag{6}$$

and

$$\eta_r = \varepsilon + \frac{\nu}{\omega_r^2} \tag{7}$$

2.2.2.1. Eigenvalues and eigenvectors

The vibration analysis (analytic, numerical or modal) aims to determine the eigenvalues (natural frequencies and damping factors) and eigenvectors (mode shapes). The eigenvalues provides information about the range of operation of a shaft, for example, and the eigenvectors helps us to understand the modal behavior of the shaft [9].

Considering the proportional damping case, the eigenvectors for a hysteretically damped system and the eigenvectors of an identical undamped system are the same, i.e., to obtain the eigenvector it is enough to solve the system shown in Equation (8).

$$det|[K] - \omega^2[M]| = 0 \tag{8}$$

Solving the system above will result on a set of N natural frequencies for the system, i.e., the eigenvalues of the undamped system. Though the eigenvalues of a undamped system are not the same as the hysteretically damped system, so, in order to determine the eigenvalues of the damped system (which has a complex form), Equation (13) must be used [9].

$$\lambda_r^2 = \bar{\omega}_r^2(1 + i\,\eta_r) \quad ; \quad \bar{\omega}_r^2 = k_r/m_r \quad \text{and} \quad \eta_r = \beta + \gamma/\bar{\omega}_r^2 \tag{9}$$

Where λ_r^2 is the damped natural frequency for the r^{th} vibration mode, $\bar{\omega}_r^2$ is the r^{th} eigenvalue squared (square of the r^{th} natural frequency mode). Calculating each r^{th} value will allow to compose the eigenvector for the hysteretically damped system.

2.2.3. Frequency response functions

Frequency response functions (FRFs) are mathematical expressions that show a direct connection between a system's modal properties and its response characteristics [9]. In modal analysis, the FRF represents the ratio between the input forces and the system's response to it. The response measured depends on which properties are desirable to obtain. Figure 3 shows a schematic representation of a measurement procedure.

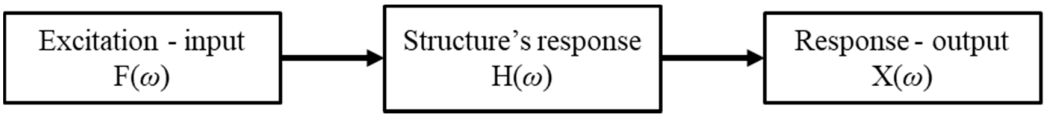

(a). Theoretical representation of an experimental measurement.

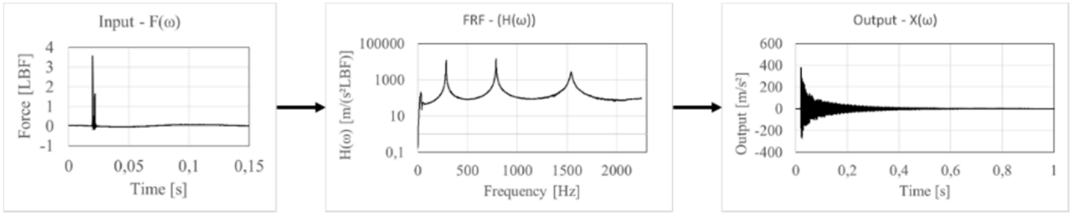

(b). Obtained signals from an experimental analysis.

Figure 3. Schematic representation of an EMA.

The FRFs commonly used in vibration analysis measures the acceleration (accelerance or inertance), velocity (mobility) and displacement (receptance) response. However, the inverse relation can be used if necessary [8]. The most common FRFs used in vibrations are displayed in Table 1.

Table 1. Definition of Frequency Response Functions [9], modified.

Response parameter	**FRF**	**Expression**	**Inverse FRF**	**Expression**
Displacement	Receptance	$H(\omega) = \frac{X}{F}$	Dynamic Stiffness	$H^{-1}(\omega) = \frac{F}{X}$
Velocity	Mobility	$Y(\omega) = \frac{V}{F}$	Mechanical Impedance	$Y^{-1}(\omega) = \frac{F}{V}$
Acceleration	Accelerance (Inheritances)	$A(\omega) = \frac{A}{F}$	Apparent Mass	$A^{-1}(\omega) = \frac{F}{A}$

where X, F, V and A are frequency domain signals, being: X the displacement response signal, F the force input signal, V the velocity response signal and A the acceleration response signal. Every FRF is frequency dependent $f(\omega)$ and a complex value (its magnitude contains information about the amplitude and phase). The receptance of the rth mode of a MDOF system with hysteretic damping is shown in Equation (13):

$$H(\omega) = \sum_{r=1}^{N} \frac{(\Psi_{jr})(\Psi_{kr})}{m_r(\omega_r^2 - \omega^2 + i\,\eta_r\,\omega_r^2)} \tag{10}$$

2.2.3.1. Reciprocity of the Frequency Response Functions

The analytical approach to the modal analysis, in most of cases, assumes that the structure obeys *Maxwell's* reciprocity principle: the response measured in a point *p* due to an input in point *q* is equivalent to the output measured in point *q* due to an identical input in point *p* [19]. When applied to a modal analysis, this assumption yields that the mass, stiffness, damping and frequency response functions matrices are symmetric.

Applying the reciprocity principle to a FRF calculated from an impact test, it implies that, at a natural frequency, the FRF measured in the DOF *p* due to an excitation in the DOF *q* is equivalent to the FRF measured in a DOF *q* due to the same excitation in the DOF *p.*

The individual FRFs measured during the tests, for a mode shape *k*, are arranged on a matrix as shown in Equation (13):

$$[H(\omega_k)] = \begin{bmatrix} H_{11}(\omega_k) & H_{12}(\omega_k) & \cdots & H_{1N_i}(\omega_k) \\ H_{21}(\omega_k) & H_{22}(\omega_k) & & H_{2N_i}(\omega_k) \\ \vdots & & \ddots & \vdots \\ H_{N_o1}(\omega_k) & H_{N_o2}(\omega_k) & \cdots & H_{N_oN_i}(\omega_k) \end{bmatrix} \quad (11)$$

Where N_i is the number of inputs and N_o is the number of outputs measured when performing the modal analysis. A SISO EMA can provide enough data to form one element, one row, one column or even the full FRF matrix, depending only of how many tests are performed on the structure under analysis. The measurements using the output as a reference and the roving excitation point provides a full row of the FRF matrix and the roving output case provides a full column.

By the *Maxwell's* reciprocity principle, an element $H_{pq}(\omega_k)$ must be equivalent to $H_{qp}(\omega_k)$, i.e., if a full row is obtained, the full equivalent column will be obtained as well or vice-versa.

2.3. Sound and Vibration

2.3.1. Definition and measurement parameters

Fahy [20] relates the sound with the variations on mass density, pressure, temperature and the particles' position of a fluid along the time. This variation are small when compared with the values it would assume on the absence of sound [20].

It is known that the propagation of a soundwave is adiabatic, i.e., the temperature gradients between the parts compressed and expanded of a fluid are too small when compared with the pressure and mass density variations. The equations describing these variations of mass density and pressure take a hyperbole form however, when analyzing acoustic signals, this equation can be approximated by a linear variation [21], [22].

The sound intensity level (SIL) is one of the main parameters to characterize an acoustic phenomenon. Using Vivolo's words [23]: "sound intensity is a vector, which expresses the magnitude and direction of the instantaneous sound power per unit of area". The sound intensity measurements can be used to locate the source and visualize sound fields [23].

2.3.2. Sound radiation in plates

The study of natural vibration modes in plates is of great concern to understand the acoustic radiation. It is known that the sound generated from a vibrating plate is composed by the sound of each mode acting on it. Some modes has more influence on the sound emitted by the plate and other ones are less significant. It happens because the sound generated by a part of the plate can be cancelled by another one vibrating with an opposite phase. Figure 4 represents the characteristic energy flux generate by the vibration of a rectangular plate in resonance, notice how some vectors are cancelled. For this case, in particular, the resulting soundwaves is composed, mostly, for the energy irradiated by the plate's extremities and that, in the near field, the sound intensity vector can be negative [24], [25].

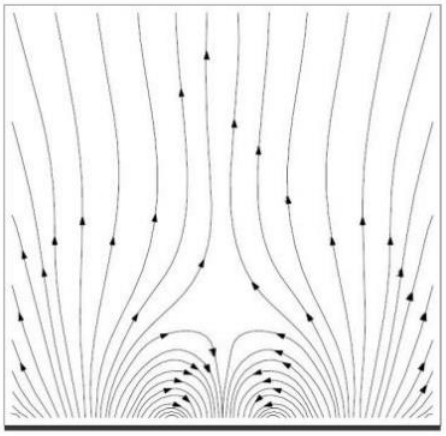

Figure 4. Characteristic energy flux irradiated by a rectangular plate in resonance [24].

The propagation of flexural waves in plates is associated with the frequency of the vibration, i.e., the flexural waves can be [25]:

1. Subsonic: the velocity of propagation for the mechanical wave is lower than the velocity of sound on the medium surrounding it. Once the equilibrium is perturbed it oscillates slower than the sound velocity of propagation, cancelling most of or even completely the sound radiation.
2. Sonic: the velocity of propagation for the mechanical wave and for the acoustic wave is the same, meaning that, when perturbed, the vibrating plate generates an acoustic wave that is parallel to the surface of the plate.

3. Supersonic: the velocity of propagation for the mechanical wave is higher than the velocity of sound on the medium surrounding it. Once the equilibrium is perturbed it oscillates faster than the sound velocity of propagation. There is no cancelling here and the intensity of the irradiated sound is much intense.

2.3.3. Correlation with vibrations

As discussed on Item 1.1, there are some situations that using accelerometers to measure a structure's output is not possible. In these situations, an acoustic approach comes up as an acceptable option in many cases.

The measurement using devices that captures the soundwaves is possible because the air is has elasticity properties, implying that, if a mass oscillate on air, a pressure response, proportional to the disturbance condition, will be presented as a reaction of the fluid medium. Assuming that the oscillating mass is represented by a vibrational system, and that the pressure variation is proportional to the amplitude of response on a natural frequency, it is possible to obtain the natural frequencies and the damping ratio of a recorded soundwave, for example [6], [7], [20].

Sometimes the acoustic approach is not possible, e.g., when the structure under analysis is heavily damped, the microphone can be unable to detect enough data, implying the impossibility to measure the natural frequencies and damping ratios required [26].

2.4. Damage and its effects

Damage affects a beam's mass and stiffness and these parameters affect, directly, the modal behavior of a system under vibration.

Take a vibrating beam, for example. Many authors describe its modal behavior (usually using Euler-Bernoulli theory for thin beams) and show that the natural frequencies and mode shapes are dependent, also, of the mass and stiffness parameters. The stiffness matrix of a simple Euler-Bernoulli element (considering transversal displacement and rotation in one plane) is given by Equation (12) [1], [3], [27].

$$[k_{el}] = \frac{EI}{l^3}\begin{bmatrix} 12 & 6l & -12 & 6l \\ & 4l^2 & -6l & 2l^2 \\ & & 12 & -6l \\ sym. & & & 4l^2 \end{bmatrix} \quad (12)$$

Where E is the Young's modulus for the material, I the inertia moment for the undamaged element and l the length of the element.

Considering the Young's modulus does not change over time, the only factor that can contribute to the change on the element's stiffness value is the inertia moment. Now, consider a damaged beam element with an I^* inertia moment (the asterisk represents the damaged condition). The new bending stiffness will be $EI^* = (EI + \Delta EI)$, where $\Delta EI = EI^* - EI$. Usually, the term ΔEI is negative, causing a decrease on the stiffness and, consequently, an increase on the flexibility on this element. The

The increase on the flexibility can imply an increase of the damping because the structure will be more susceptible to plastic deformation and an increase on its internal friction [3].

The damage detection and location has been an interesting study field recently. Pandey and Biswas [28] tried to detect damage using the changes in the flexibility matrix, latter, Bernal [29], [30] proposed a method to locate the damage based on the change of the flexibility matrix. Ewins [9] developed a method to detect damage based on changes on the stiffness matrix. Stubbs *et al.* [31] developed the method to detect and locate damage based on strain energy. His work were used by Worden *et al.* [32] and Maeck [33] to continue and develop this studies.

2.5. Structure Health Monitoring

Structure Health Monitoring (SHM) is the process of implementing a damage detection and characterization strategy for structures, machines and systems [34]. SHM's main goal is to provide a diagnosis of the condition of the constituent materials, the parts of the structure (boundary conditions, connectivity, etc.) and the full assembly as a whole, making possible to keep the structural state inside the limits specified during the structure's design. The usage of SHM also makes possible to obtain a prognosis (evolution of damage and residual life, for example) of the structure [3].

To diagnosis about the health condition of a structure requires obtaining data about it. The data acquisition system must be designed defining the sensors, selected according to the physical phenomenon under analysis, the locations to place them, the number of sensors to be used, the data processing (acquisition, transmission and storage) hardware and how often the system must acquire data from the sensors used [3], [34].

Though the monitoring system is not cheap, there are some benefits of using SHM. Using the SHM system on a machine of the manufacturing sector as an example, allows an optimal usage of the machine. Also turns possible to reduce the downtime, by planning more exactly the maintenance program or even replacing the scheduled and periodic stops by performance-based or condition-based data analysis in long term or avoiding the disassemble of part of it searching for a non-existing problem, in short term. SHM also reduces the human interference during the machine's operation, avoiding human errors and incident risks provoking an increase on the safety and reliability of the process. The data collected using SHM, along with a well planned maintenance program using the SHM data can avoid a catastrophic failure of the machine [3].

Some examples of systems that use SHM systems are military vehicles, army systems, civil aircrafts and civil infrastructures, preventing accidents, failures and improving the safety of the operation. In fact, SHM helped to decrease the amount of aircrafts accidents caused by failures of maintenance and structural weaknesses. In 2006 only 14% of hull loss aircraft accidents are due to failure on maintenance and 4% are due to structural weakness (excluding sabotage and military actions cases), proving that the SHM system helps to improve safety and reliability of the system [3].

Usually, along the lifetime of a machine, the reliability decreases and the maintenance cost increases. Using SHM system allows to maintain constant or minimize the variation of these values along the machine's lifetime [3].

SHM can be passive or active. Passive SHM means that the system is only under monitoring but no action is taken (to monitor the acoustic emissions, for example). Active SHM means that the monitoring is providing information and some action is taken if necessary [3].

2.6. Model updating

When an engineer designs a structure, he also designs a model of the structure. Usually simulations are performed to check if the theoretical data agrees with the expected. These tests can be performed using a prototype of the structure, using a finite element simulation, etc. The cost to simulate the structure's behavior is lower when compared to the cost of building the structure and test under operation.

Though simulations are a good way of verifying the theoretical data, sometimes, the results are not enough accurate to be used as a guarantee. These inaccuracies may happen for some reasons; including a bad model generated during the design stage (the model can use wrong boundary conditions, idealized geometry, inadequate material properties, etc.) or some errors during the measurement part. A possibility that can try and, in many cases, solve the inaccuracies problem is using a model updating method [3].

Model updating method is used to locate and correct some errors that may have occurred during the design of the model used in the finite element (FE) analysis or to locate some parameters, boundary conditions, type of element used, etc. that can be changed to increase the model's accuracy.

3. MATERIALS AND METHOD

3.1. Materials and geometries

The beams used in the practical part of this work are made of the Aluminum alloy 6082 and its relevant properties are available in Table 9, on APPENDIX A.

The beams have parallelepiped format and its dimensions are available in the design schematics on APPENDIX A.

The damage infliction was simulated by perforations. The diameter values used for each test are available in Table 2.

Table 2. Perforation dimensions used.

Beam nº	Perforation diameter [mm]						
	Test 1	Test 2	Test 3	Test 4	Test 5	Test 6	Test 7
1	0	15	16	17	18	19	20
2	0	21	22	23	24	25	26
3	0	27	28	29	30	31	32
4	0	33	34	35	36	37	38

The damage changes the moment of inertia and the mass of the beam, affecting the values of the natural frequencies of the system. Table 3 shows the calculated impact of the damages on the mass (*m*), moment of inertia (*I*) and the expression *(EI/m)* (the beam's bending stiffness per unit of mass), where *E* is the Young's modulus of the material.

It is worth remembering that $I = bh^3/12$, where b is the unaffected width (40 mm for the undamaged condition and 40-*d* for the damaged condition) and h the height (5 mm) of the beam. The value presented on Table 3 refers to the center of the beam, where it is most affected by the damage inflicted. It is possible to obtain this value for other position long the beam.

The variations (Δ) were obtained using the undamaged value as the reference and it is an absolute value but represents a decrease on its value.

"NA" stands for "not applicable".

Table 3. Impact of the damage on the mass and moment of inertia of the analyzed beams.

d [mm]	*m* [kg]	*Δm* [%]	*I* [x10^{-11} m^4]	*ΔI* [%]	*EI/m* [m^3/s^2]	*Δ(EI/m)* [%]
0	0,1626	NA	41,6667	NA	179,3768	NA
15	0,1602	1,47	26,0417	37,50	113,7861	36,57
16	0,1599	1,68	25,0000	40,00	109,4601	38,98
17	0,1595	1,89	23,9583	42,50	105,1302	41,39
18	0,1592	2,12	22,9167	45,00	100,7947	43,81
19	0,1588	2,36	21,8750	47,50	96,4517	46,23
20	0,1583	2,62	20,8333	50,00	92,0996	48,66
21	0,1579	2,89	19,7917	52,50	87,7363	51,09
22	0,1574	3,17	18,7500	55,00	83,3602	53,53
23	0,1570	3,46	17,7083	57,50	78,9693	55,98
24	0,1565	3,77	16,6667	60,00	74,5616	58,43
25	0,1559	4,09	15,6250	62,50	70,1353	60,90
26	0,1554	4,42	14,5833	65,00	65,6882	63,38
27	0,1548	4,77	13,5417	67,50	61,2184	65,87
28	0,1543	5,13	12,5000	70,00	56,7237	68,38
29	0,1536	5,50	11,4583	72,50	52,2020	70,90
30	0,1530	5,89	10,4167	75,00	47,6511	73,44
31	0,1524	6,29	9,3750	77,50	43,0687	75,99
32	0,1517	6,70	8,3333	80,00	38,4525	78,56
33	0,1510	7,13	7,2917	82,50	33,8000	81,16
34	0,1503	7,57	6,2500	85,00	29,1089	83,77
35	0,1496	8,02	5,2083	87,50	24,3765	86,41
36	0,1488	8,48	4,1667	90,00	19,6002	89,07
37	0,1480	8,96	3,1250	92,50	14,7773	91,76
38	0,1472	9,45	2,0833	95,00	9,9050	94,48

To facilitate the measuring procedure a grid was drawn, each square's side is one centimeter long and the grid was drawn using a permanent marker, avoiding damage infliction and mass loading to the beam. An example with the grid drawn can be seen in Figure 5.

3.2. Methods

The following topics will describe the methods and procedures adopted to accomplish the numerical and experimental analysis used in this work.

3.2.1. Numerical method

In order to obtain the expected modal parameters to the beams under testing, a FEM modal analysis was performed to each beam in every case scenario (undamaged and damaged).

During the development of the numerical method, two software programs were used: SolidWorks and Ansys.

The numerical approach starts with the beams' design using the SolidWorks (v. 2016) software and, subsequently, the FEM simulations were performed using Ansys' (v. 18.2) "Modal Testing" package. The goal is to obtain the numerical modal parameters of the structures (natural frequencies and mode shapes) for a "free" support condition.

The numerical analysis was set to obtain the mode shapes and its corresponding natural frequency for a free vibrating condition, on a range from zero to 2000 Hz. The first six vibration modes corresponds to rigid body motion and were discarded. The remaining vibration modes were used as an expected value to the experimental testing.

3.2.2. Experimental method

The purpose of the experimental method is to obtain the natural frequencies and the damping ratio of the structure and is divided in two steps: impact test using an accelerometer to measure the output signal (accelerometer method); and impact test using a sound level meter to measure the output data (sound level meter method).

The undamaged beams were tested individually and their natural frequencies and damping ratios were obtained for each test method (using accelerometers and sound level meter). During the tests using the accelerometer method the output was also measured using the sound level meter in order to compare and validate the obtained data. After, the beams were perforated, on its center (as can be seen in APPENDIX A), tested again (using both methods) and the process repeats five more times, always

increasing the damage diameter in 1 millimeter each time. The dimensions of all perforations are available on the Table 2.

The dimensions of the holes simulate a wide range of damage severity levels, going from a low severity level (the second test of the beam number one) to a high severity level (the seventh test of the beam number 4). This allows verifying how this damage affects the modal properties and, consequently, the modal behavior of the structure under analysis.

To make easier to refer to the testings, the notation used is: $T_{n,m}$, where: n is the tested beam's number and m refers to the test number. For example $T_{3,4}$ refers to the fourth test for the beam number three, i.e., the beam with a 29 mm perforation.

The beams were tested on a foam surface, simulating a "free" support condition.

An impact hammer (model E086C40) was used to provide the input signal. All the beams were impacted at the same location, as represented in Figure 5-a.

However, the usage of the impact hammer combined with the points adopted, fails to obtain enough data about the torsional and transversal modes of vibration. Therefore, aiming to obtain the torsional vibration mode, four tests ($T_{3,2}$, $T_{4,3}$, $T_{1,7}$ and $T_{4,7}$) were performed using alternative input and output measurement points (see Figure 5-b). The discussion is available on the results analysis chapter.

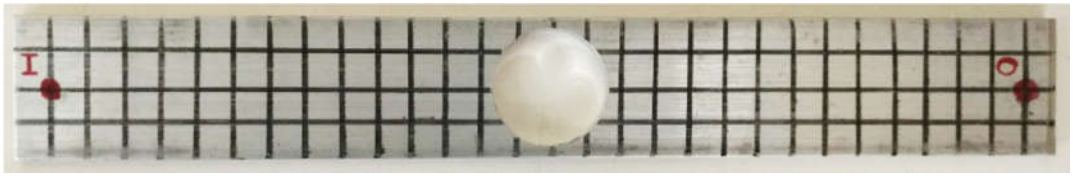

(a). Excitation and output points to every test. Where "I" represents the excitation, or input, point and "O" represents the output point).

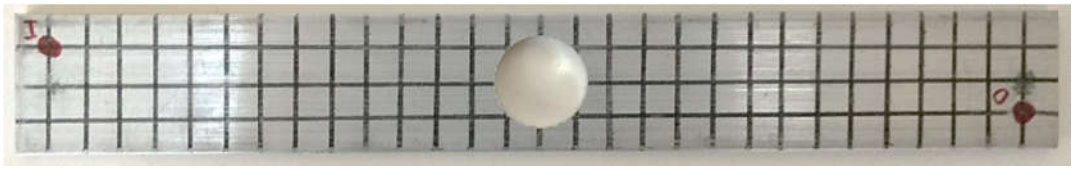

(b). Excitation and output points to the specific tests. Where "I" represents the excitation, or input, point and "O" represents the output point).

Figure 5. Excitation and output points.

3.2.2.1. Impact testing using accelerometers

The impact testing for modal analysis using an accelerometer to measure the output signal is an EMA testing and aims to obtain the system's response to a known force input (impact excitation). The analysis of the obtained data allows determining the experimental modal parameters of the structure under test. The parameters measured in this work, however, are limited to the natural frequencies and damping ratios.

To avoid measurement errors and to stablish a standard parameter to the measurements, two points were chosen to be the standard reference points to the input (impact) and the output (accelerometer). The location of the points will not change during the damage infliction and will be used to every measurement, in every test. In addition, four tests were performed using additional reference points, aiming to obtain the torsional natural frequency on the range under analysis. Looking at Figure 5 it can easily be seen the difference between the reference points used on each test.

A uniaxial accelerometer (type 4508, manufactured by Brüel & Kjær) was used to measure the response signal. The accelerometer was plugged to a PHOTON+ dynamic signal analyzer and the analyzer is connected to a PC using an USB cable. The data was processed using the RT Pro Photon software (v. 7.30.01).

At first, a SISO roving hammer impact test and a roving accelerometer impact test were performed in the undamaged beams, aiming to demonstrate the reciprocity of the FRF matrix. During the first test the roving input case was assumed, the accelerometer was taken as the reference for the FRF, i.e., it was fixed. After, the roving output case was assumed, meaning that the impact point was used as the reference to the FRF, which implies that the impact occurred always in the input point and the accelerometer was moved to every point on the beam. A three impacts average composed the final FRF for each point.

The roving tests have the purpose to measure two sets of FRFs. By comparing the sets obtained it can be ssen that the FRF matrix is reciprocal, i.e., the output measured on node i when the beam is impacted on node j should show the same behavior if the beam was impacted on node i and the output was on node j.

The previous test also provides enough data to obtain the modal shapes of the system, however, this approach was not considered on this work due to the lack of software available.

After the roving test, the impact tests using SISO were performed. To improve the accuracy and obtain a more reliable result, the tests results considered an average of five data samples. Now the impacts were the input and the response the output. Figure 6 shows a representation of the tests performed on the beams.

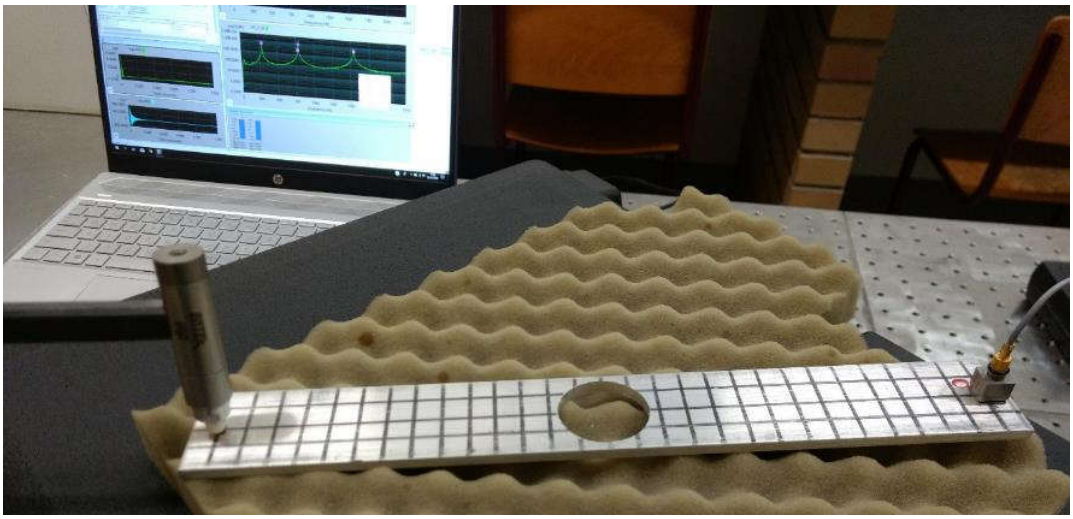

(a). Representation of a standard test using an accelerometer as an output source.

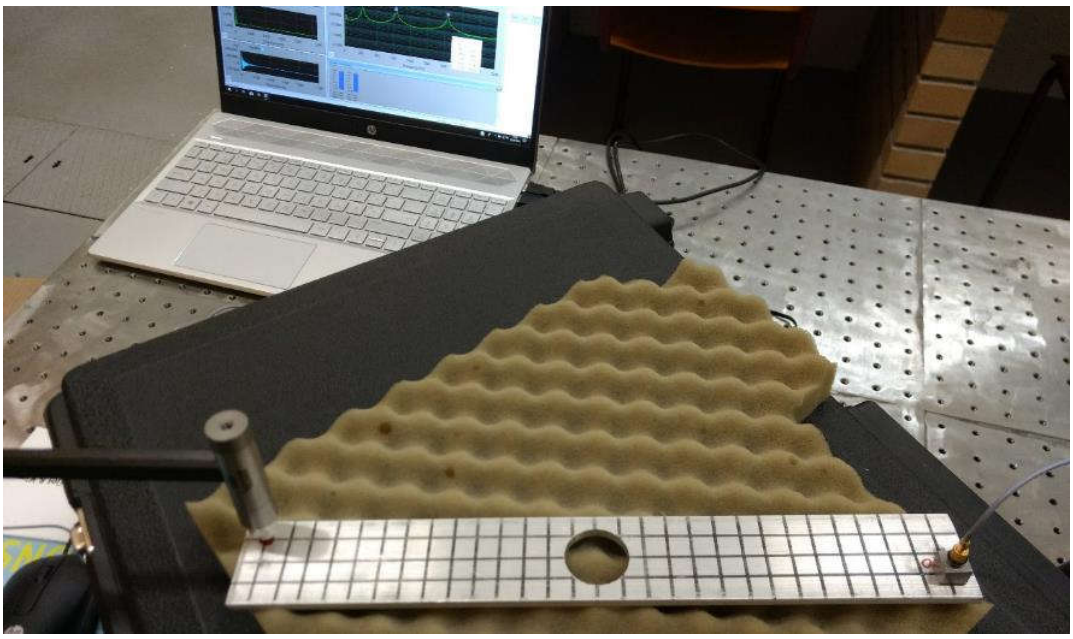

(b). Representation of a test to obtain the torsional natural frequencies.

Figure 6. Impact test using an accelerometer as an output source.

3.2.2.2. Impact testing using a sound level meter

The impact testing to obtain the frequency response using a sound level meter to measure the output data is an impact test that aims to obtain the system's sound response to a known force input (impact excitation). The analysis of the obtained data allows determining the experimental natural frequencies and damping coefficient of the structure under test.

Following the previous method, two points were chosen to be the standard reference points to the input and the output; also, the location of the points will not change during the damage infliction and will be used to every measurement, in every test. Using the sound level meter method discards the need to change the output point (as in the previous case) because the soundwaves are affected by the transversal behavior (it will be discussed on the discussion section). However, every accelerometer test using the transversal reference points were performed using the sound level meter as well, providing enough data to compare and validate the previous tests. Figure 5 shows the reference points used on each test.

A Hand-held analyzer (type 2250, G-4, manufactured by Brüel & Kjær), equipped with a ½ inch, pre-polarized, free-field microphone (type 4189, manufactured by Brüel & Kjær) was used to record, process and analyze the structure's acoustic response. In addition, a MATLAB code was used to perform a FFT on the obtained sound signal and provide the natural frequencies.

Just like in previous case, the beam was excited in the input point. For the tests using only the sound level meter to measure the output data, the microphone was positioned vertically, perpendicular to the surface of the beam, above the output point (5 cm distant) and the structure was impacted. An exemplification can be observed in Figure 7.

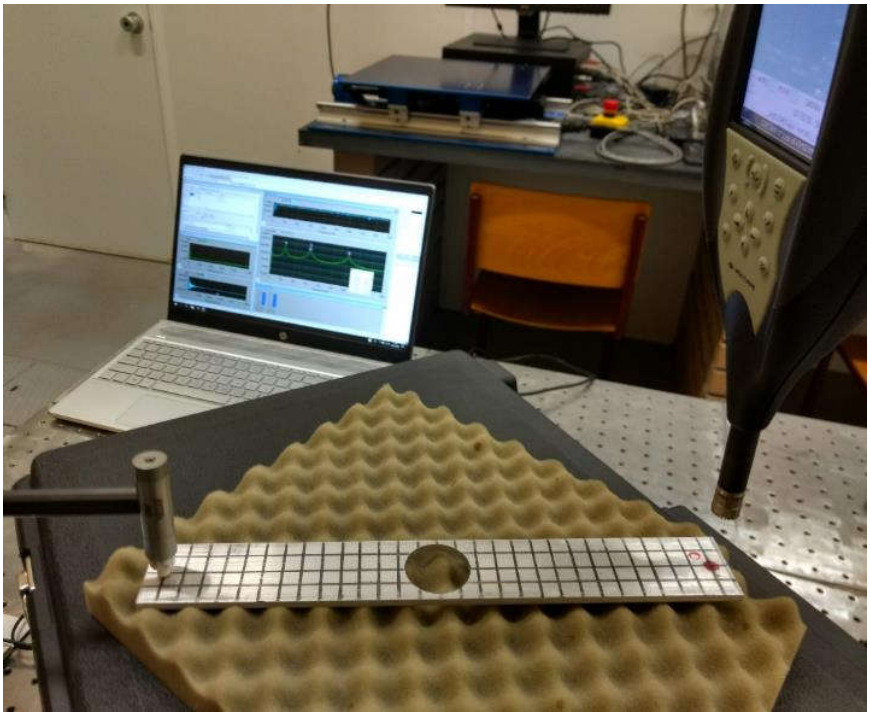

(a). Representation of a standard test using a sound level meter as an output source.

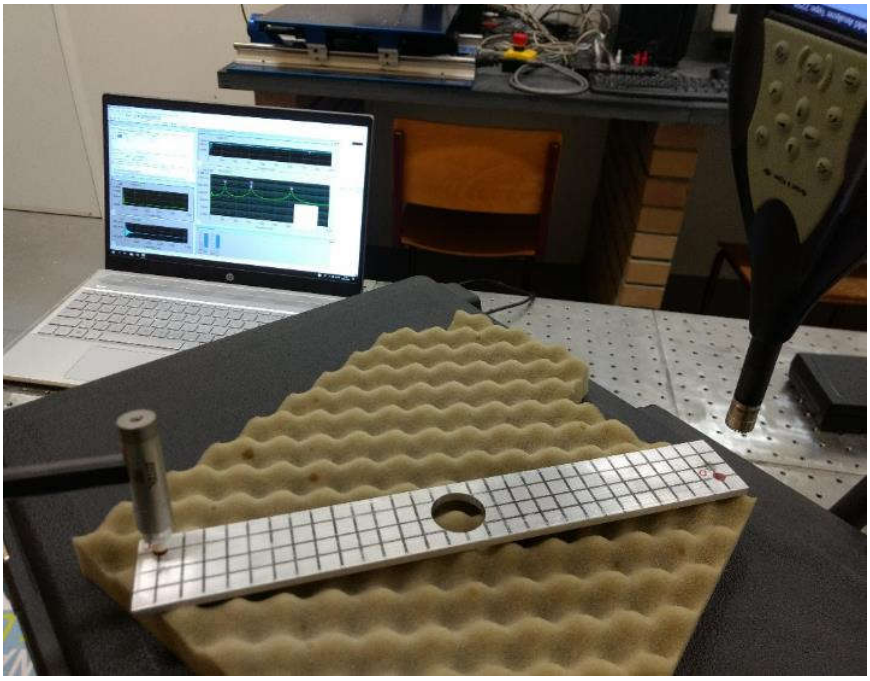

(b). Representation of the test performed to validate the results.

Figure 7. Impact test using a sound level meter as an output source.

The hand-held analyzer processed the recorded signal, providing the frequency spectrum, obtained using a FFT analyzer package and it was used to estimate the natural

frequencies and damping ratios. The equipment used allows saving the soundwave of the recorded data. The soundwaves were processed by a MATLAB code to measure the natural frequency and compare with the ones obtained by the sound level meter's software.

4. RESULTS AND ANALYSIS

In this section, the results are presented and commented.

4.1. Beam number 1

The numerical simulation resulted four natural frequencies and mode shapes on the interval under analysis (0 to 2000 Hz). The impact tests performed also allows obtaining the damping ratio to each natural frequency (using half bandwidth method). The variation of the natural frequencies estimated by the numerical simulation and measured by the impact tests using the accelerometer and the sound level to measure the output data are available on section 4.1.1, the mode shapes on section 4.1.2 and the damping ratios on section 4.1.3.

4.1.1. Natural frequencies

Figure 8-(a) shows the variation of the estimated and measured natural frequencies of the vibration mode number one along the tests performed on the beam number one. It is simple to observe that its value drops along the tests performed (with exception of T5, it will be forward discussed), as expected, according to the numerical simulation.

Similarly, Figure 8-(b) represents the variation of the estimated and measured natural frequencies of the second vibration mode along the tests performed. It is noticeable that this frequency is not as affected by the damage inflicted as the first one (the difference between the frequency measured in tests number one and seven is less than 5 Hz). It is also possible to see that not every test obtained the result corresponding to the expected decrease on the natural frequency (T5, T6 and T7 using the accelerometer to measure the output data and T6 using the sound level meter to measure the output data).

Figure 8-(c) shows the variation of the estimated and measured natural frequency of the third vibration mode along the tests performed. This frequency, in particular, has data obtained only by the numerical simulation and the measurements using the sound level meter (it will be discussed ahead). It is possible to notice that the natural frequencies change according to expected, decreasing along the tests.

Finally, Figure 8-(d) shows the variation of the estimated and measured natural frequencies of the fourth vibration mode along the tests performed. Again, the results obtained using the sound level meter to measure the output data obey the expected behavior (decreases along the tests) and there is one result measured, using the accelerometer to measure the output data, that is not according to expected (T7 natural frequency increases instead of decreasing).

The errors between the estimated values and the measured values are available on Table 4.

Table 4. Errors between the measured values using the accelerometer and the sound level meter for Beam number one.

	Error [%]						
	T1	T2	T3	T4	T5	T6	T7
ω_{n1}	4,605	4,279	4,506	5,232	4,319	4,588	4,629
ω_{n2}	3,810	3,810	3,968	4,140	3,901	3,981	3,809
ω_{n3}	NA	NA	NA	NA	NA	NA	NA
ω_{n4}	3,759	3,060	4,150	4,090	4,236	4,377	3,423

It is worth remembering that the error was calculated using the expression:

$$Error = 100\frac{\left|\omega_{ni,acel} - \omega_{ni,slm}\right|}{\omega_{ni,acel}} \quad (13)$$

Where $\omega_{ni,acel}$ is the value of the i^{th} natural frequency measured using the accelerometer to measure the output data, $\omega_{ni,slm}$ is the i^{th} natural frequency measured using the sound level meter as a to measure the output data and $i=1,2,3,4$. It is noticeable that the reference value used is the obtained with the accelerometer. NA stands for “not applicable”.

The table with all the errors associated with beam number one are available at APPENDIX B.

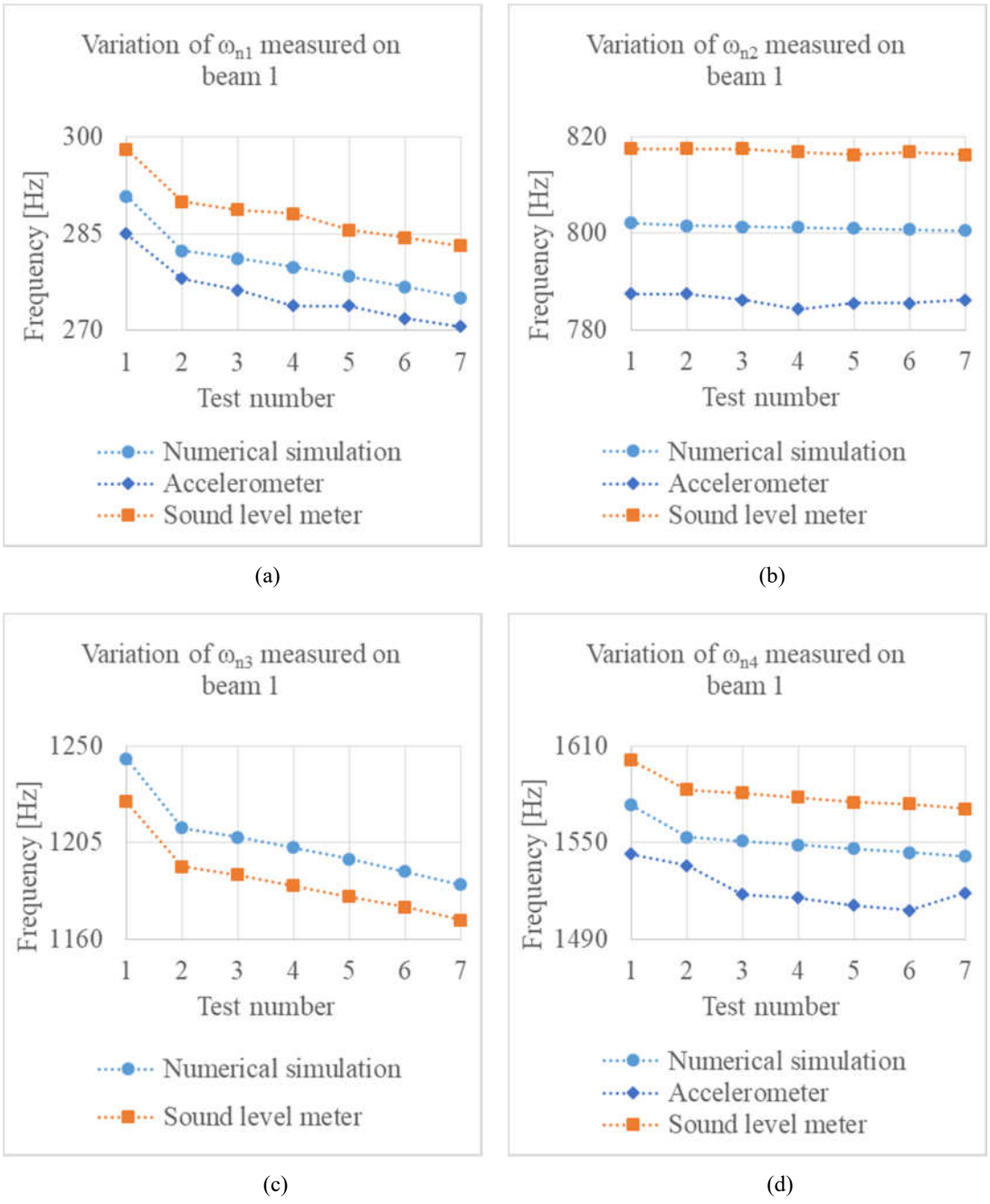

Figure 8. Estimated and measured frequencies for beam number one.

4.1.2. Mode shapes

The mode shapes were obtained during the modal analysis performed using Ansys. The numerical analysis was performed using 2 mm elements and using the

mechanical APDL solver for the eigenvalue problem.. For the beam number one there are four mode shapes relevant to the results (see Figure 9).

Figure 9-(a) shows the first mode shape for the beam number one (flexural mode number one), (b) shows the second mode shape (flexural mode two), (c) shows the third mode shape (torsion mode number one) and (d) shows the fourth mode shape (flexural mode number three). The values of the frequencies for each mode shape are the ones estimated by the numerical simulation, for the beam number one the values obtained from $T_{1,1}$ simulation were used.

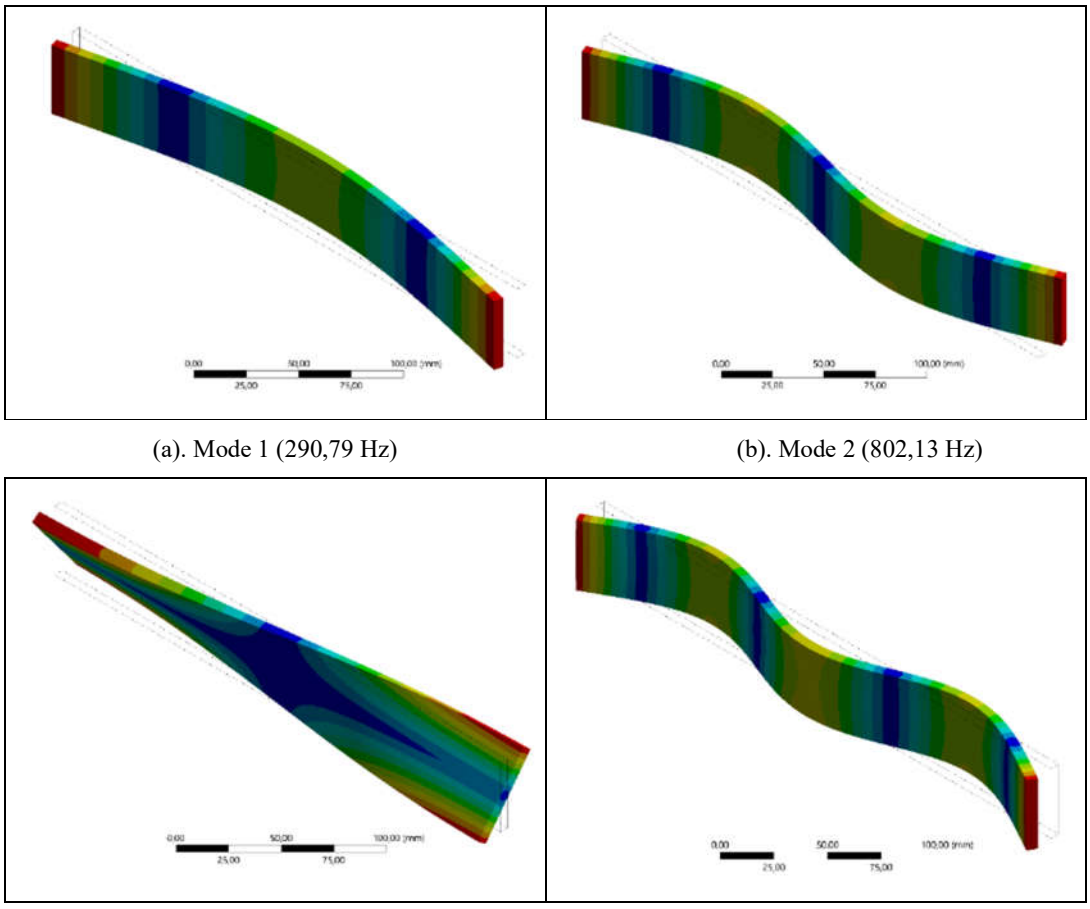

(a). Mode 1 (290,79 Hz) (b). Mode 2 (802,13 Hz)

(c). Mode 3 (1244 Hz) (d). Mode 4 (1573,3 Hz)

Figure 9. Mode shapes obtained for the beam number one.

4.1.3. Damping ratios

The damping ratios are relevant modal properties to be analyzed. The values for the damping ratio presented bellow were measured using the half bandwidth method on the data obtained during the impact tests using the accelerometer to measure the output data. Figure 10 shows the variation of the damping ratio along the tests performed on beam number one, using the accelerometer to measure the output data.

DR stands for "damping ratio" and the number after it refers to the number of the mode associated to its value (e.g., DR_1 is the damping ratio for the first vibration mode).

It is noticeable that the values for the damping of the first mode increase along the tests, while the ones associated with the second does not change significantly and the DRs associated with the fourth vibration mode varies a lot (it will be discussed on the next chapter).

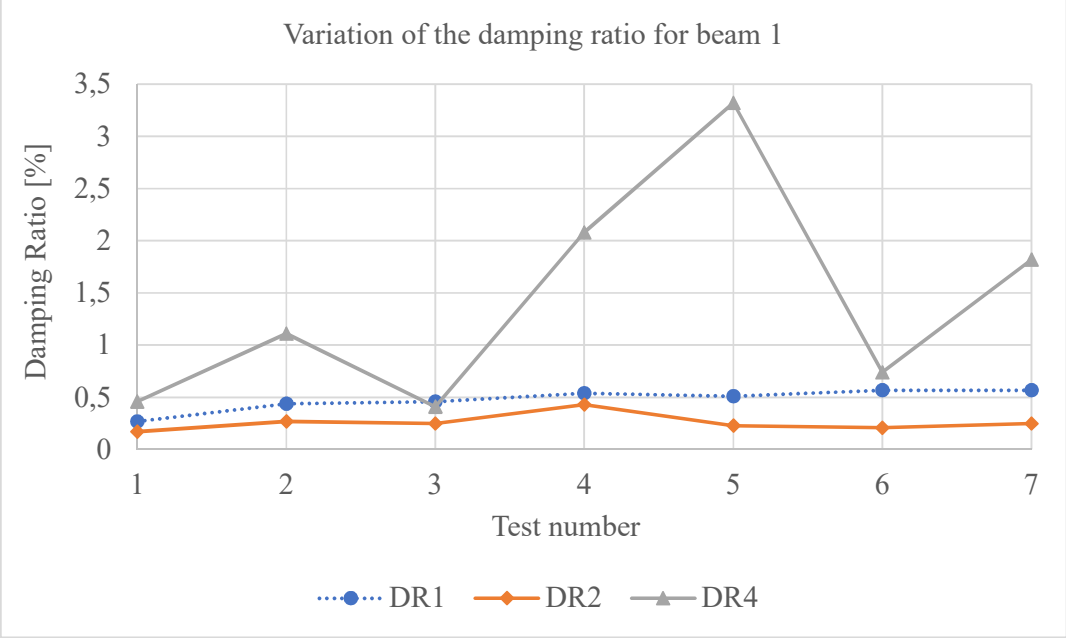

Figure 10. Damping ratios measured for beam number one.

4.2. Beam number 2

The numerical analysis performed on beam number two also resulted four natural frequencies and mode shapes on the frequency range under analysis. The impact tests performed also allow obtaining the damping ratio to each natural frequency. The variation of the natural frequencies estimated by the numerical simulation and measured by the impact tests using the accelerometer and the sound level meter to measure the output data are available on section 4.2.1, the mode shapes on section 4.2.2 and the damping ratios on section 4.2.3.

4.2.1. Natural frequencies

Figure 11-(a) shows the variation of the estimated and measured natural frequencies of the vibration mode number one along the tests performed on the beam number two. It is simple to observe that its value drops along the tests performed, as expected, according to the numerical simulation.

Similarly, Figure 11-(b) represents the variation of the estimated and measured natural frequencies of the second vibration mode along the tests performed. It is noticeable that this frequency is not as affected by the damage inflicted as the first one (similarly to the results obtained from beam number one, the difference between the frequency measured in tests number one and seven is less than 5 Hz). It is also possible to see that not every test obtained the result corresponding to the expected (the natural frequencies of the tests T5, T6 and T7, using the accelerometer as the output source and T7 using the sound level meter increase instead of decreasing).

Figure 11-(c) shows the variation of the estimated and measured natural frequencies of the third vibration mode along the tests performed. This frequency, in particular, has data obtained only by the numerical simulation and the measurements using the sound level meter (it will be discussed ahead). It is possible to notice that the natural frequencies decrease, according to expected.

Finally, Figure 11-(d) shows the variation of the estimated and measured natural frequencies of the fourth vibration mode along the tests performed. Again, the results obtained using the sound level meter to measure the output data obey the expected behavior and there are two results obtained, using the accelerometer to measure the output data, that are not according to expected (T3 and T7).

The errors between the estimated values and the measured values are available on Table 5.

The calculation method used was the same used in 4.1.1. NA stands for “not applicable”.

The table with all the errors associated with beam number two are available at APPENDIX B.

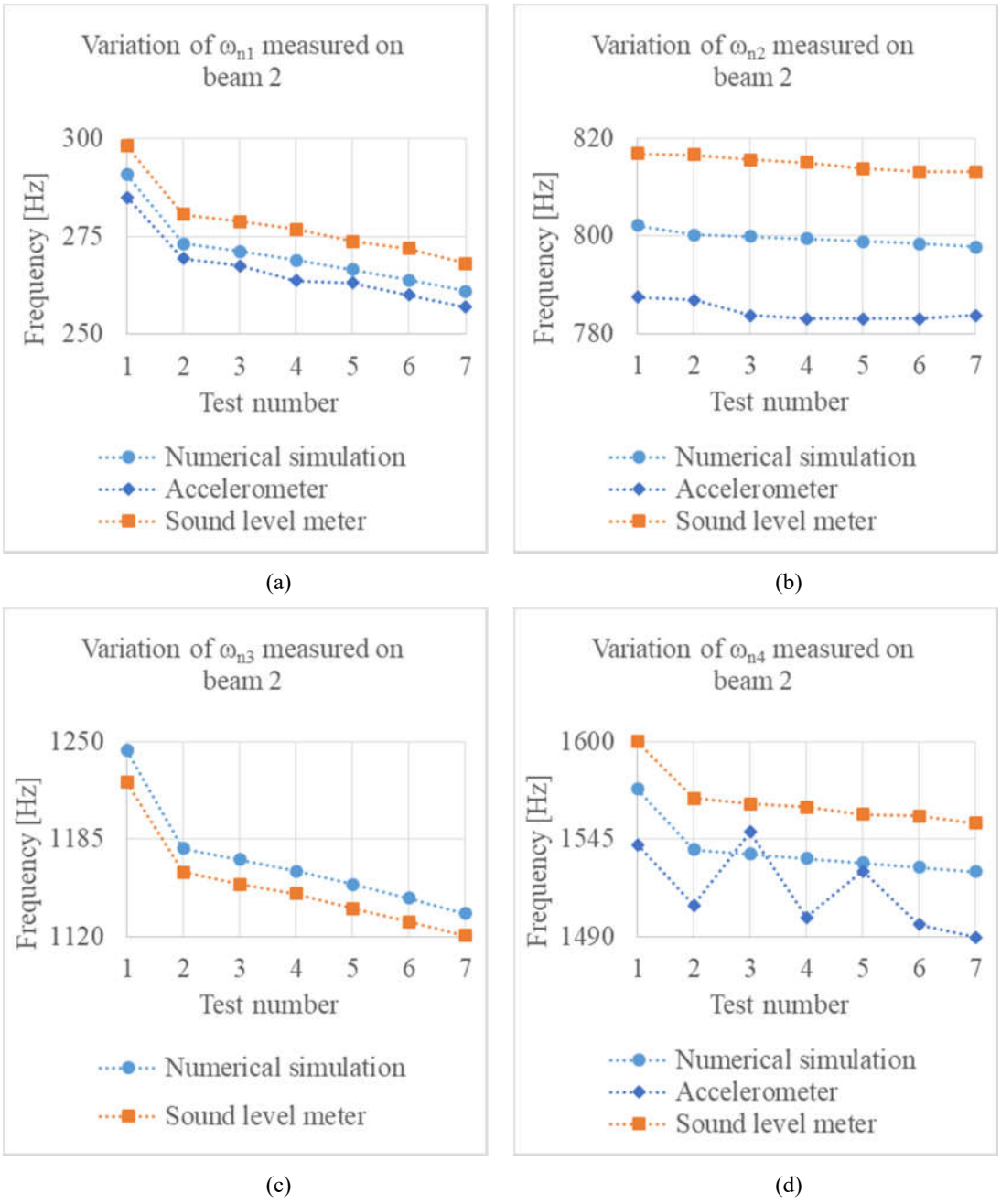

Figure 11. Estimated and measured frequencies for beam number two.

Table 5. Errors between the measured values using the accelerometer and the sound level meter for Beam number two.

	Error [%]						
	T1	T2	T3	T4	T5	T6	T7
ω_{n1}	4,605	4,167	4,206	4,956	4,048	4,567	4,369
ω_{n2}	3,730	3,777	4,060	4,074	3,914	3,834	3,741
ω_{n3}	NA	NA	NA	NA	NA	NA	NA
ω_{n4}	3,761	3,979	1,033	4,131	2,096	4,075	4,295

4.2.2. Mode shapes

The mode shapes were obtained during the modal analysis performed using Ansys. To beam number two four mode shapes were obtained on the frequency range under analysis (see Figure 12).

Figure 12-(a) shows the first mode shape for the beam number two (flexural mode number one), (b) shows the second mode shape (flexural mode two), (c) shows the third mode shape (torsion mode number one) and (d) shows the fourth mode shape (flexural mode number three). The values of the frequencies for each mode shape are the ones estimated by the numerical simulation, for the beam number two the values obtained on $T_{2,2}$ were used as an example.

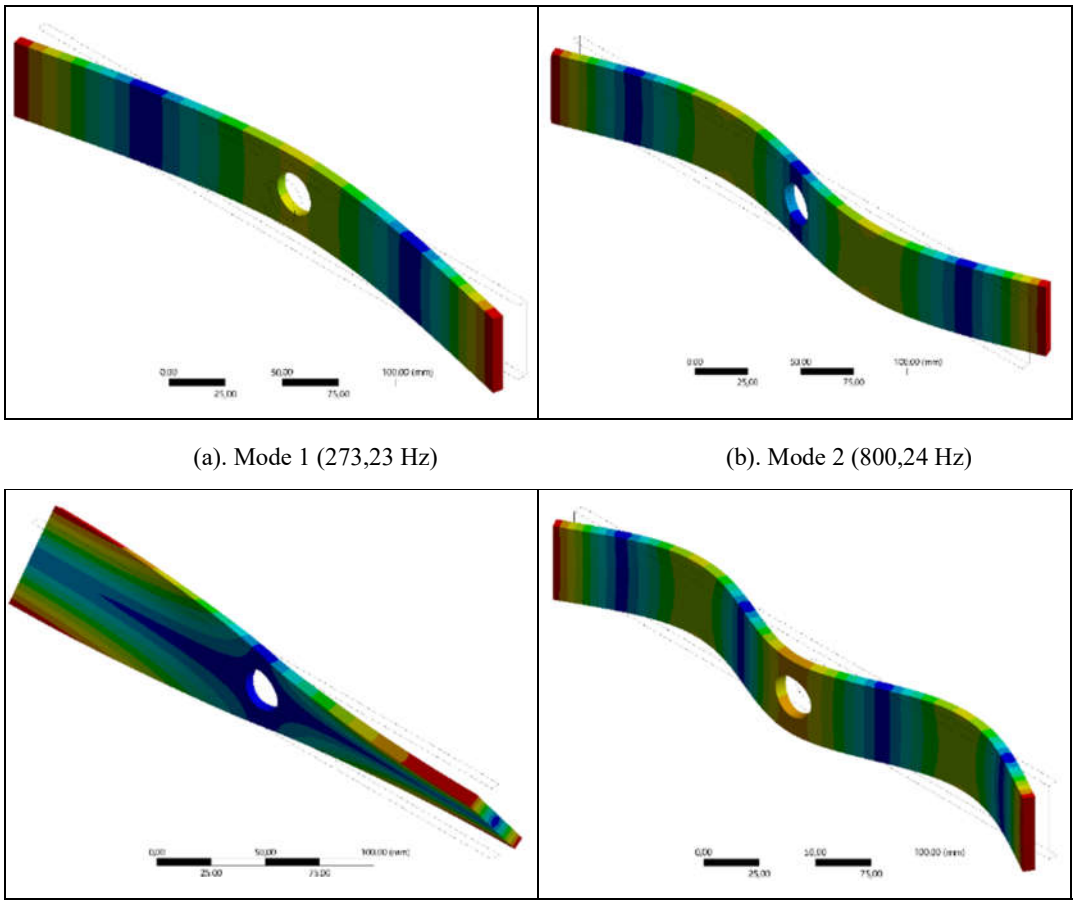

(a). Mode 1 (273,23 Hz) (b). Mode 2 (800,24 Hz)

(c). Mode 3 (1178,88 Hz) (d). Mode 4 (1539,2 Hz)

Figure 12. Mode shapes obtained for the beam number two.

4.2.3. Damping ratios

Figure 13 shows the variation of the measured damping ratios along the tests performed on beam number two, using the accelerometer to measure the output data.

It is noticeable that the values for the damping of the first mode increase along the tests, while the ones associated with the second does not change significantly and the DRs associated with the fourth vibration mode oscillates (it will be discussed on the next chapter).

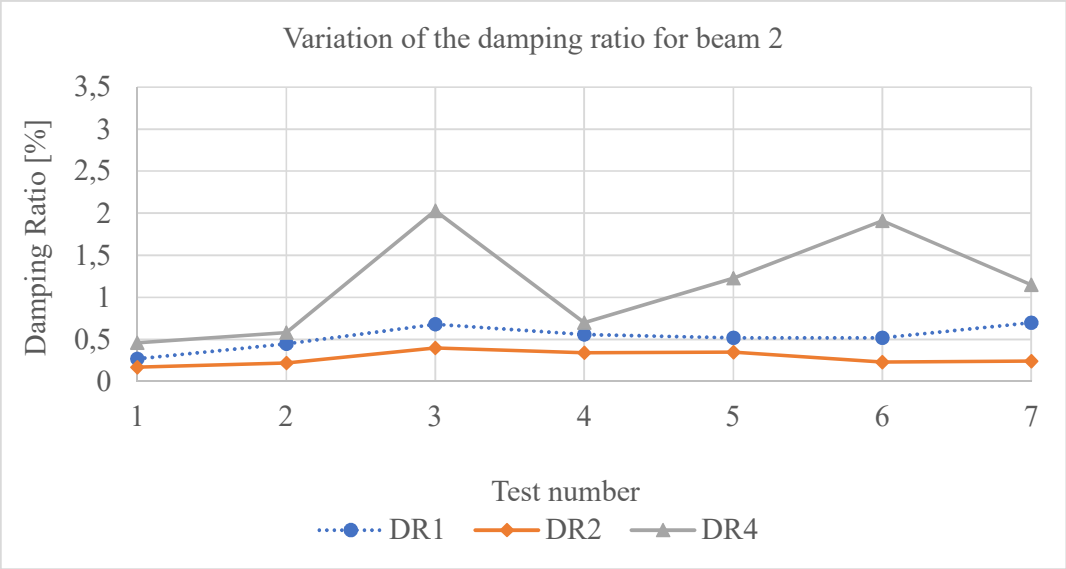

Figure 13. Damping ratios measured for beam number two.

4.3. Beam number 3

For beam number three, the numerical simulation also resulted four natural frequencies and mode shapes on the frequency range under analysis. The impact tests performed allowed obtaining the damping ratio to each natural frequency. Following the same sequence used previously, the variation of the natural frequencies estimated by the numerical simulation and measured by the impact tests using the accelerometer and the sound level meter to measure the output data are available on section 4.3.1, the mode shapes on section 4.3.2 and the damping ratios on section 4.3.3.

4.3.1. Natural frequencies

Figure 14-(a) shows the variation of the estimated and measured natural frequencies of the vibration mode number one along the tests performed on the beam number three. It is simple to observe that its value drops along the tests performed, as expected, according to the numerical simulation.

Similarly, Figure 14-(b) represents the variation of the estimated and measured natural frequencies of the second vibration mode along the tests performed. It is noticeable that this frequency is not as affected by the damage inflicted as the first one

(similarly to the results obtained from beam number one, the difference between the frequency measured in tests number one and seven is less than 5 Hz). It is also possible to see that not every test obtained the result corresponding to the expected (the natural frequency value for the tests 3 and 7 increases, on the tests performed using the accelerometer to measure the output data).

Figure 14-(c) shows the variation of the estimated and measured natural frequency of the third vibration mode along the tests performed. This frequency, in particular, has data obtained only by the numerical simulation and the measurements using the sound level meter (it will be discussed ahead). It is possible to notice that the natural frequencies change according to the values obtained with the numerical simulation.

Finally, Figure 14-(d) shows the variation of the estimated and measured natural frequency of the fourth vibration mode along the tests performed. Again, the results obtained using the sound level meter to measure the output data obey the expected behavior (decrease along the tests) and there are two results obtained, using the accelerometer to measure the output data, that are not according to expected (T3 and T7).

The errors between the estimated values and the measured values are available on Table 6.

The calculation method used was the same used in 4.1.1. NA stands for “not applicable”.

The table with all the errors associated with beam number three are available at APPENDIX B.

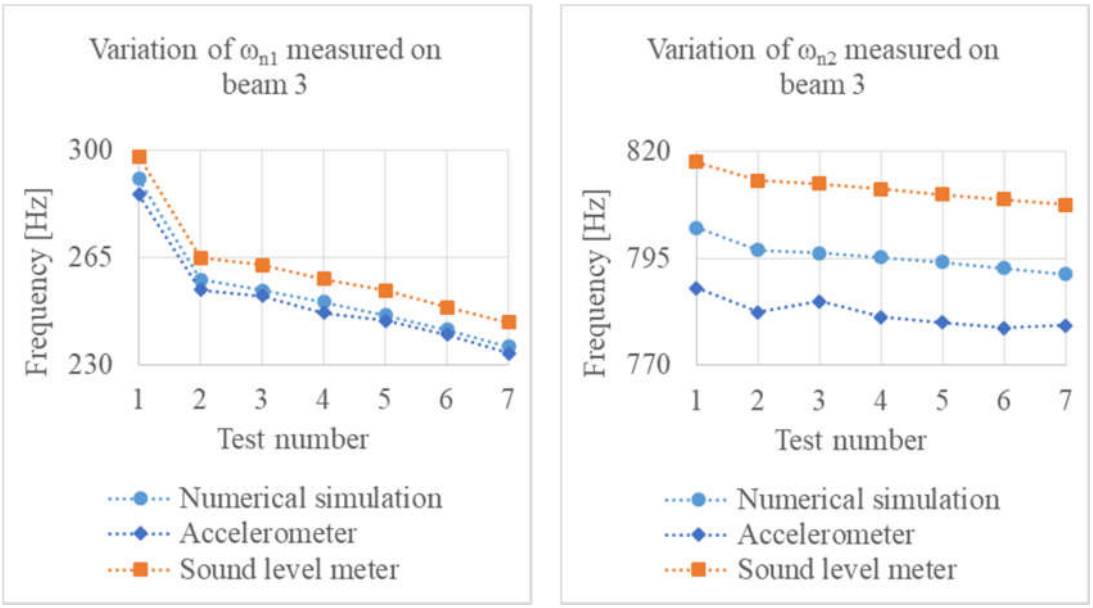

(a) (b)

(c) (d)

Figure 14. Estimated and measured frequencies for beam number three.

Table 6. Errors between the measured values using the accelerometer and the sound level meter for Beam number three.

	Error [%]						
	T1	T2	T3	T4	T5	T6	T7
ω_{n1}	4,386	4,167	3,960	4,546	4,081	3,732	4,256
ω_{n2}	3,730	3,914	3,503	3,833	3,846	3,846	3,605
ω_{n3}	NA	NA	NA	NA	NA	NA	NA
ω_{n4}	3,891	4,155	3,536	4,030	4,248	4,113	2,188

4.3.2. Mode shapes

The mode shapes were obtained during the modal analysis performed using Ansys. For the beam number three four mode shapes were obtained on the frequency range under analysis (see Figure 15).

Figure 15-(a) shows the first mode shape for the beam number three (flexural mode number one), (b) shows the second mode shape (flexural mode two), (c) shows the third mode shape (torsion mode number one) and (d) shows the fourth mode shape (flexural mode number three). The values of the natural frequencies for each mode shape are the ones estimated by the numerical simulation, for the beam number three the values obtained on $T_{3,2}$ were used as an example.

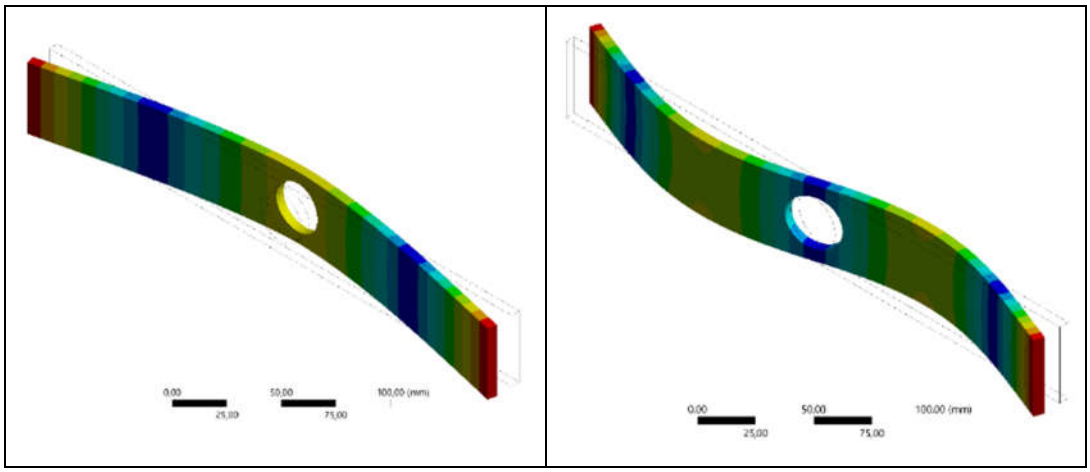

(a). Mode 1 (257,87 Hz) (b). Mode 2 (797,03 Hz)

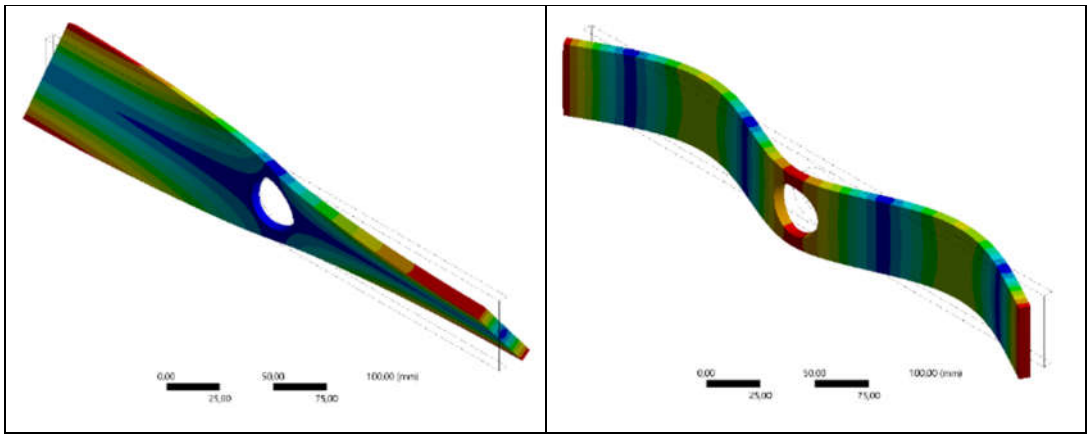

(c). Mode 3 (1124,6 Hz) (d). Mode 4 (1524,4 Hz)

Figure 15. Mode shapes obtained for the beam number three.

However, the data obtained in numerical simulation brings an interesting result out of the frequency range under analysis: the sixth mode shape was, so far, the second torsional mode but, on $T_{3,3}$, this mode shape changes to the fourth flexural mode, as can be seen on Figure 16.

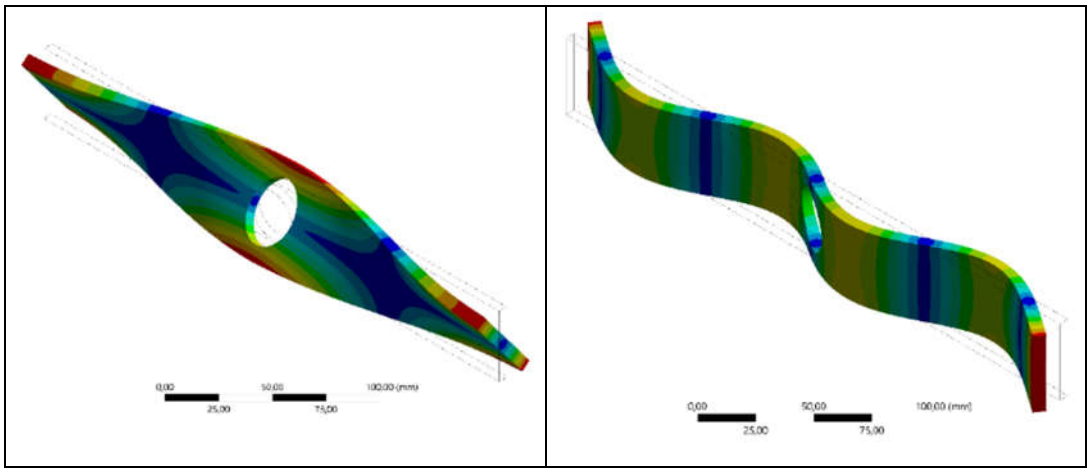

(a). Mode 6 (2548,1 Hz) for $T_{3,2}$. (b). Mode 6 (2549,2 Hz) for $T_{3,3}$.

Figure 16. Sixth mode shape to $T_{3,2}$ and $T_{3,3}$.

4.3.3. Damping ratios

Figure 17 shows the variation of the measured damping ratios along the tests performed on beam number three, using the accelerometer to measure the output data.

The values measured for the damping of the first mode increase along the tests (oscillating during some tests), while the ones associated with the second does not change significantly (except for the value obtained for the test number seven) and the DRs associated with the fourth vibration mode oscillates during the tests (it will be discussed on the next chapter).

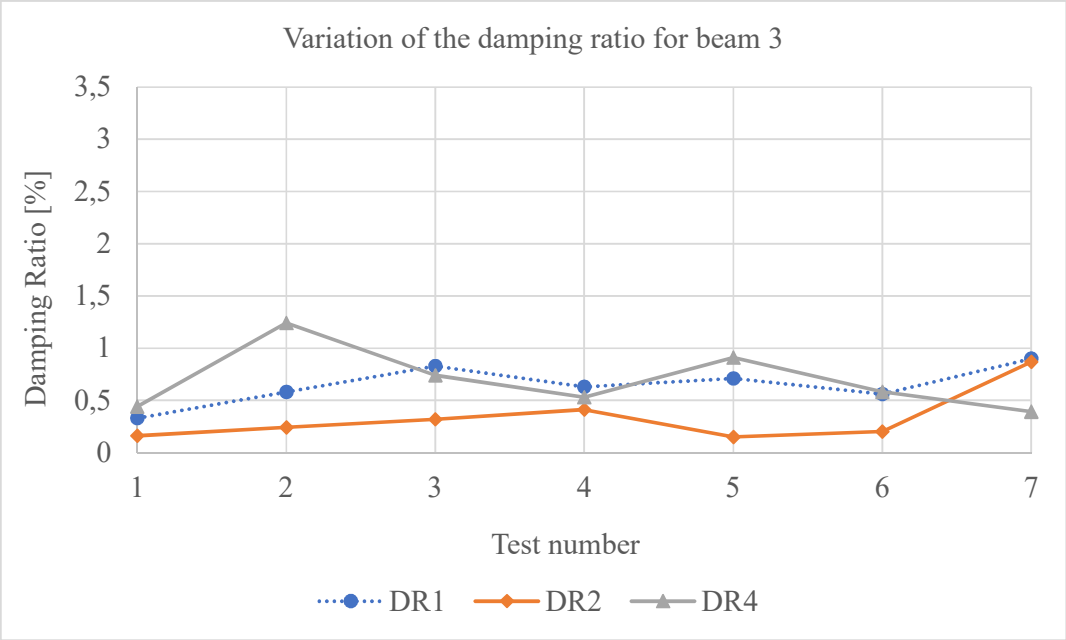

Figure 17. Damping ratios measured for beam number three.

4.4. Beam number 4

For beam number four, the numerical simulation resulted four natural frequencies and mode shapes on the frequency range under analysis until the third test ($T_{4,3}$). The simulation of the fourth and fifth tests ($T_{4,4}$ and $T_{4,5}$) resulted five natural frequencies and mode shapes on the same range. Finally, the sixth and seventh tests ($T_{4,6}$ and $T_{4,7}$) resulted six natural frequencies and mode shapes estimated on the specified range. The impact tests performed allowed obtaining the damping ratio to some natural frequencies. Following the same sequence used previously, the variation of the natural frequencies estimated by the numerical simulation and measured by the impact tests using the accelerometer and the sound level meter to measure the output data are available on section 4.4.1, the mode shapes on section 4.4.2 and the damping ratios on section 4.4.3.

4.4.1. Natural frequencies

Figure 18-(a) shows the variation of the estimated and measured natural frequencies of the vibration mode number one along the tests performed on the beam

number four. It is simple to observe that its value drops along the tests performed, as expected, according to the numerical simulation, just like in previous beams.

Similarly, Figure 18-(b) represents the variation of the estimated and measured natural frequencies of the second vibration mode along the tests performed. It is possible to see that one test did not obtain the expected result (the natural frequency value for the test 5 does not decreases, on the tests performed using the accelerometer to measure the output data).

Figure 18-(c) shows the variation of the estimated and measured natural frequency of the third vibration mode along the tests performed. Again, this frequency, in particular, has data obtained only by the numerical simulation and the measurements using the sound level meter (it will be discussed ahead). It is possible to notice that the natural frequencies change according to the values obtained with the numerical simulation, except for the sixth test, which has a greater value associated with the natural frequency.

Finally, Figure 18-(d) shows the variation of the estimated and measured natural frequency of the fourth vibration mode along the tests performed. Again, the results obtained using the sound level meter to measure the output data obey the expected behavior (a decrease on its value) and there are two results obtained, using the accelerometer to measure the output data, that are not according to expected (T5 and T7).

Although there are five natural frequencies on the fourth and fifth tests, the fifth natural frequency could not be measured on this test because it has a transversal mode shape (see Figure 20) and it is not measured by the uniaxial accelerometer used on the tests, with the points and directions adopted during the impact tests.

Similarly, on the tests number six, the natural frequencies associated with the fourth and sixth mode shapes were not measured for the same reason. Yet, on test seven, the natural frequencies of the fifth and sixth mode shapes were not detected because they are related to the transversal vibration mode.

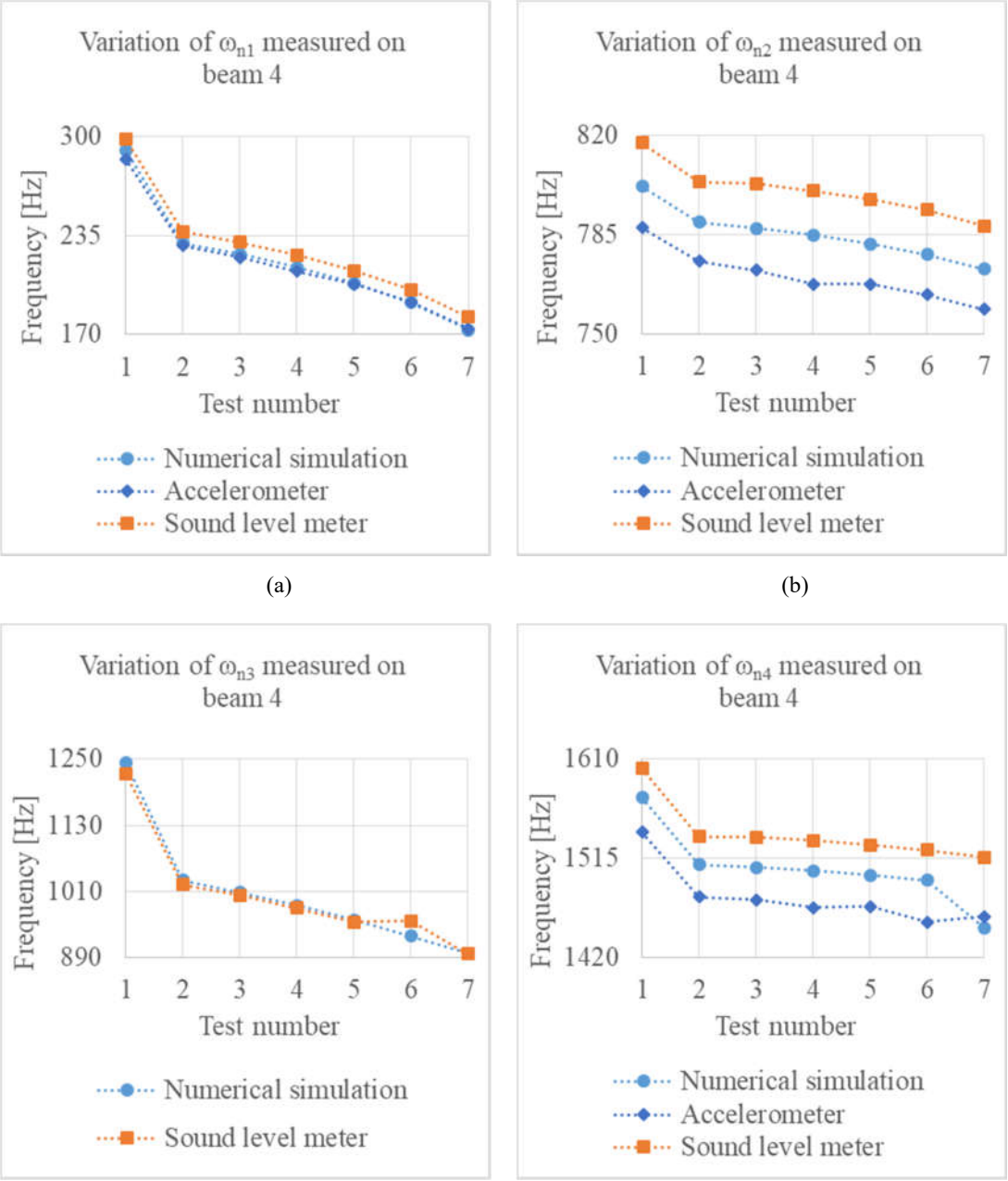

Figure 18. Estimated and measured frequencies for beam number four.

The errors between the estimated values and the measured values are available on Table 7.

The calculation method used was the same used in 4.1.1. NA stands for “not applicable”.

The table with all the errors associated with beam number four are available at APPENDIX B.

Table 7. Errors between the measured values using the accelerometer and the sound level meter for Beam number four.

	Error [%]						
	T1	T2	T3	T4	T5	T6	T7
ω_{n1}	4,605	4,121	4,544	5,005	4,321	4,221	4,287
ω_{n2}	3,810	3,629	3,964	4,316	3,909	3,921	3,865
ω_{n3}	NA	NA	NA	NA	NA	NA	NA
ω_{n4}	3,961	3,924	4,068	4,360	4,016	4,746	3,907

4.4.2. Mode shapes

The mode shapes were obtained during the modal analysis performed using Ansys. As discussed above, the numerical simulation on beam number four obtained between four and six mode shapes on the frequency range under analysis (see Figure 19 and Figure 20).

Figure 19-(a) shows the first mode shape for the beam number four (flexural mode number one), (b) shows the second mode shape (flexural mode two), (c) shows the third mode shape (torsion mode number one) and (d) shows the fourth mode shape (flexural mode number three), these results are valid until test number six.

The values for each natural frequency associated to the mode shape are the ones estimated by the numerical simulation, for the beam number four the values obtained on $T_{4,2}$ were used as an example.

As mentioned before, some mode shapes change when the severity of the damage increases. Specifically, on the test number seven, the fourth mode shape changes to the transversal mode (see Figure 20) and the third flexural mode shape becomes the fifth mode acting on the beam.

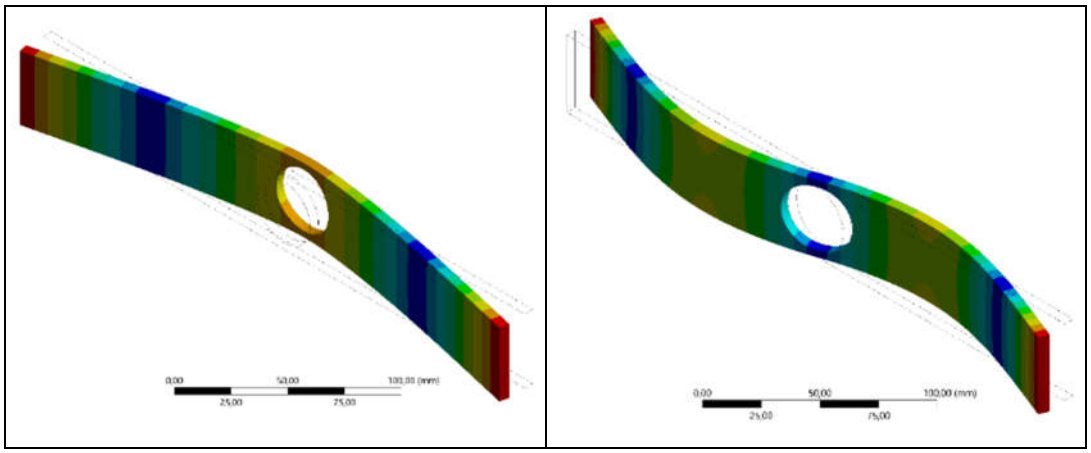

(a). Mode 1 (229,76 Hz) (b). Mode 2 (789,52 Hz)

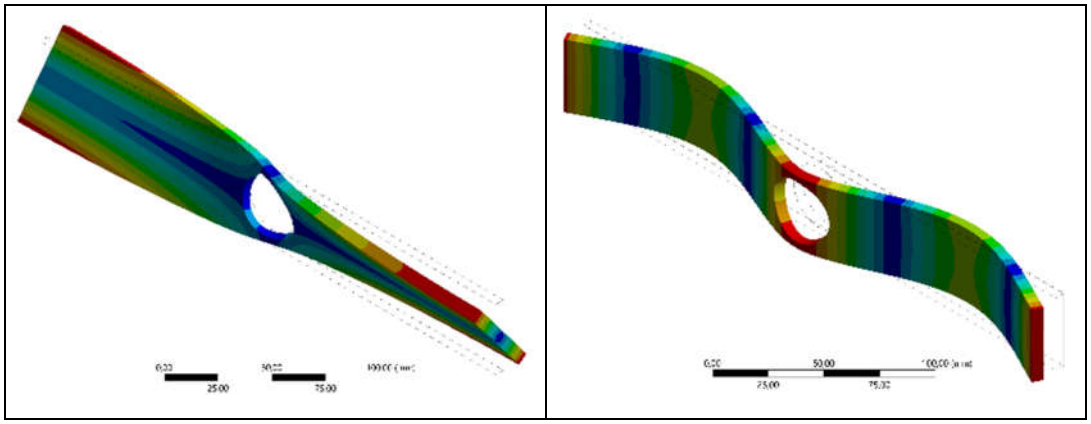

(c). Mode 3 (1030,5 Hz) (d). Mode 4 (1509,1 Hz)

Figure 19. Mode shapes obtained for the beam number four (test one to six).

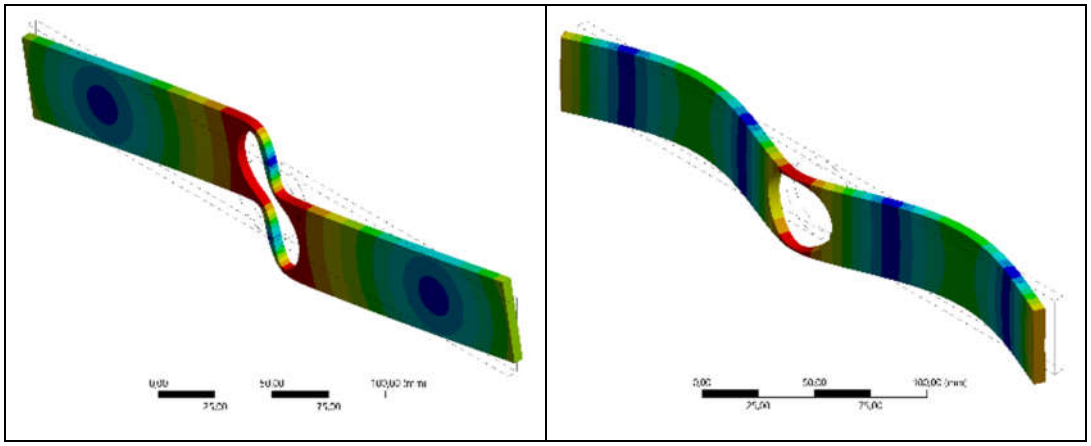

(a). Mode 4 (1448,3 Hz) (b). Mode 5 (1486,8 Hz)

Figure 20. Fourth and fifth mode shapes for test number seven on beam number four.

Yet, there is a sixth mode shape with the natural frequency value under 2000 Hz (see APPENDIX B)

4.4.3. Damping ratios

Figure 21 shows the variation of the measured damping ratios along the tests performed on beam number four, using the accelerometer to measure the output data.

The values for the damping of the first mode increase along the tests (oscillating on test number four). The damping ratios associated with the second vibration mode does not change significantly and the DRs associated with the fourth vibration mode increase along the tests.

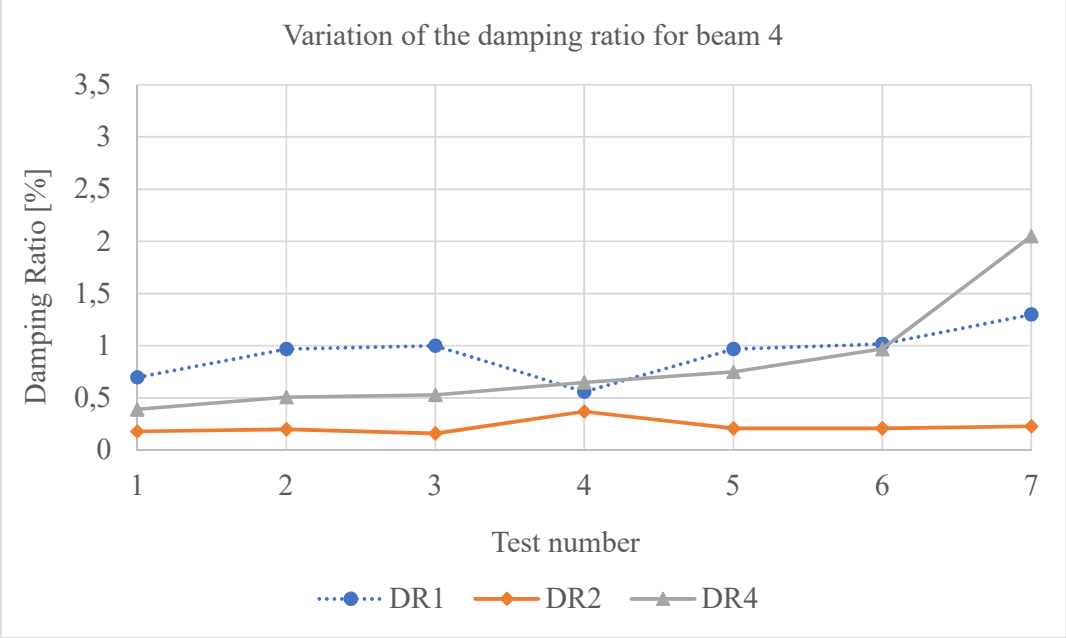

Figure 21. Damping ratios measured for beam number four.

4.5. Impact tests to determine the torsional natural frequency

Analyzing the mode shapes above allows noticing that, for every case under analysis, the third mode shape is the first torsional mode. It implies that, the input and output points used for the analysis (see Figure 5-a) are not ideal to obtain the output data to measure this mode because the accelerometer is located on a modal line where

the displacement caused by the vibrational response of the beam is not enough to allow measuring its natural frequency.

Though the accelerometer's size is not negligible on the structure under analysis (meaning that the accelerometer does obtain some data about the vibrational response), the displacement amplitudes measured by it does not allow to measure the third natural frequency for the system under analysis.

Using the sound level meter, however, allows to obtain this parameter, once the sound response is not as affected as the measured using the accelerometer, if the accelerometer is not used, i.e., during the tests using only the sound level meter to measure the output data, it is possible to measure the third natural frequency.

To obtain data and compare with the numerical simulations, four tests were performed using the Figure 5-b set of points to the input and output data measurement. The input and output points used allows to measure the torsional response of the beam because they are located at a point where the displacement is not negligible. These tests aimed to obtain the third natural frequency of the system and demonstrate that this is, indeed, a torsional frequency.

The results obtained using this set of points were measured performing tests for four cases: $T_{3,2}$, $T_{1,7}$, $T_{4,7}$ and $T_{4,3}$. The results obtained for the third natural frequency in these cases are presented in Table 8. On this table, the Error 1 is the error between the estimated values for the natural frequency (during the numerical simulation) and the measured values for the natural frequency (using the accelerometer to measure the output data. Error 2 refers to the error between the estimated values for the natural frequency (during the numerical simulation) and the values measured by the sound level meter to measure the output data.

It is worth remembering that the third natural frequency obtained during $T_{4,7}$ is not well defined (the damping factor is too big) and it is more an estimative than a real measured natural frequency.

Table 8. Values estimated and measured for ω_{n3}.

	ω_{n3} [Hz]				
Case	Numerical simulation	Accelerometer	Sound level meter	Error 1 [%]	Error 2 [%]
$T_{3,2}$	1124,6	1056	1111	6,100	1,209
$T_{4,3}$	1008,4	942,5	1003	6,535	0,536
$T_{1,7}$	1185,5	1105	1168	6,790	1,476
$T_{4,7}$	897,45	860,6	896,25	4,106	0,134

It is possible to notice a similar situation to the fourth and fifth modes of the seventh test on beam number four (4^{th} and 5^{th} modes of $T_{4,7}$ – see Figure 20). The resulting mode for the fourth mode shape does not allow to be measured by the accelerometer used. However, this time, because the vibration happens on a transversal direction and the accelerometer used is uniaxial, i.e., measure the response in one direction, only. To measure the natural frequencies associated to these mode vibrations it should either be used a bi or tridimensional accelerometer or change its orientation. However, for this specific case, no extra tests were performed.

4.6. Global results

This section aims to show the variation of the natural frequencies and the damping ratios along all the tests performed on the beams.

The impact tests performed on the beams are planned to be continuous, i.e., the diameter of the last test performed on beam number one ($T_{1,7}$, 20 mm diameter) has the dimension immediately below the diameter of the second test performed on beam number two ($T_{2,2}$, 21 mm diameter, because the $T_{2,1}$ is the test performed on the undamaged beam). The same is valid for all the other last tests of every beam. This sequence of testing allows analyzing the variation of the natural frequencies and damping ratios along all the severity levels of the damage inflicted to the beam.

4.7. Natural frequency

The X axis values are planned to separate every beam, i.e., the first interval (X index one to seven) represents the first seven tests performed on beam number one ($T_{1,x}$), the second interval represents the six tests performed on the damaged beam number two ($T_{2,x-7}$) and so on.

Figure 22 shows the variation of the first natural frequency estimated and measured during the tests.

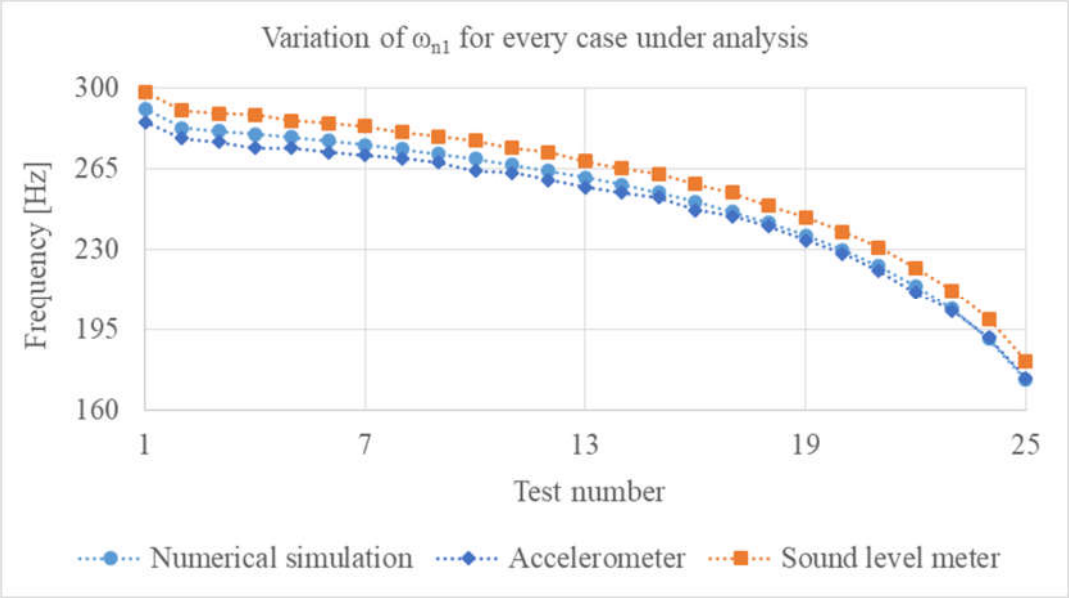

Figure 22. Global analysis of the first natural frequency variation along the tests.

Similarly, Figure 23 shows the variation of the second natural frequency estimated and measured during the tests.

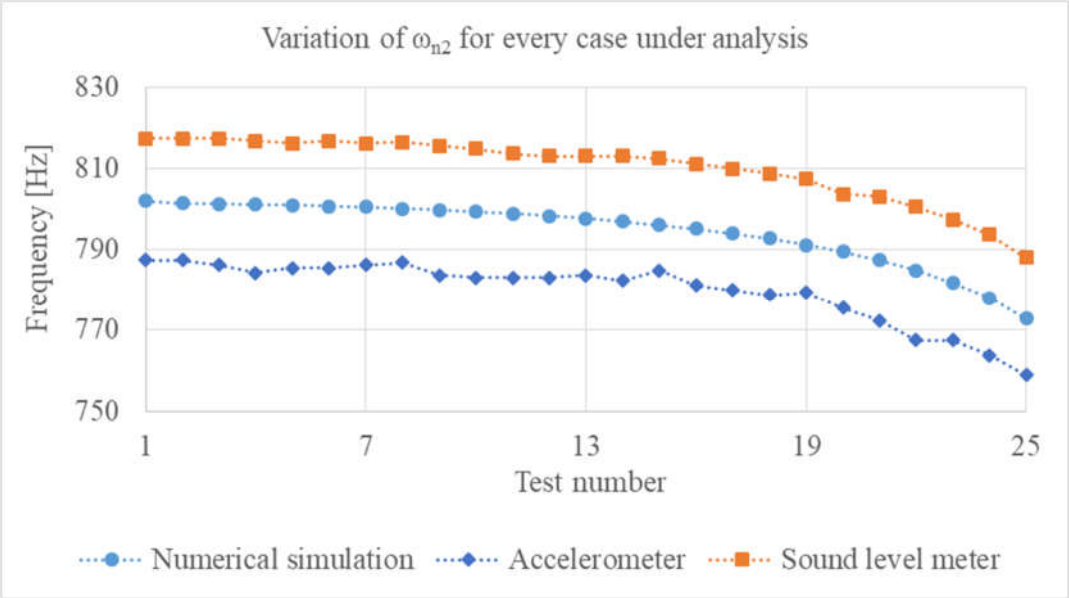

Figure 23. Global analysis of the second natural frequency variation along the tests.

Figure 24 shows the variation of the third natural frequency estimated and measured during the tests.

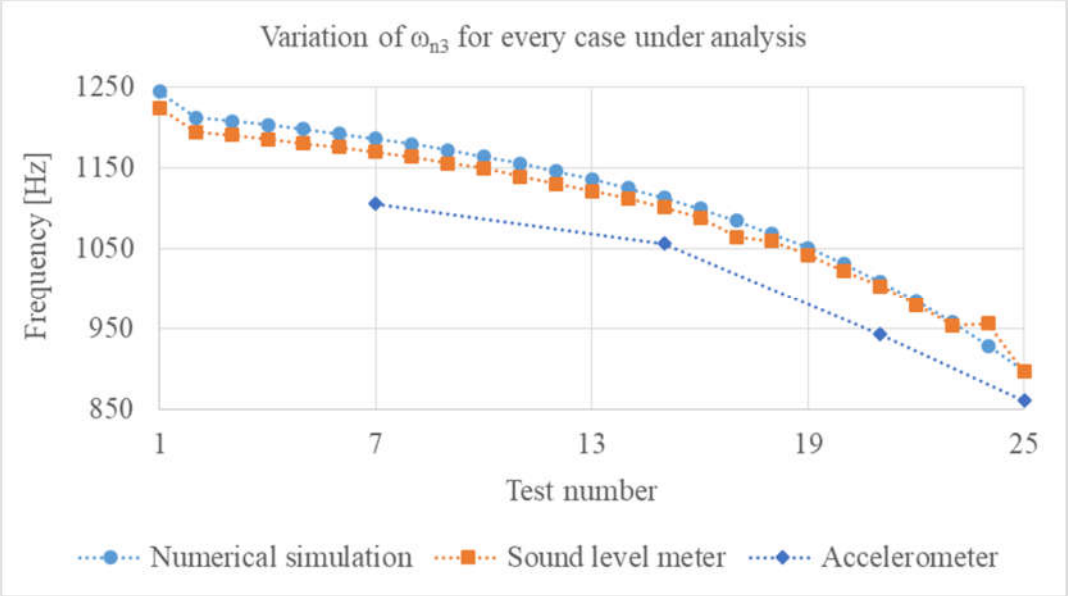

Figure 24. Global analysis of the third natural frequency variation along the tests.

Figure 25 shows the variation of the fourth natural frequency estimated and measured during the tests.

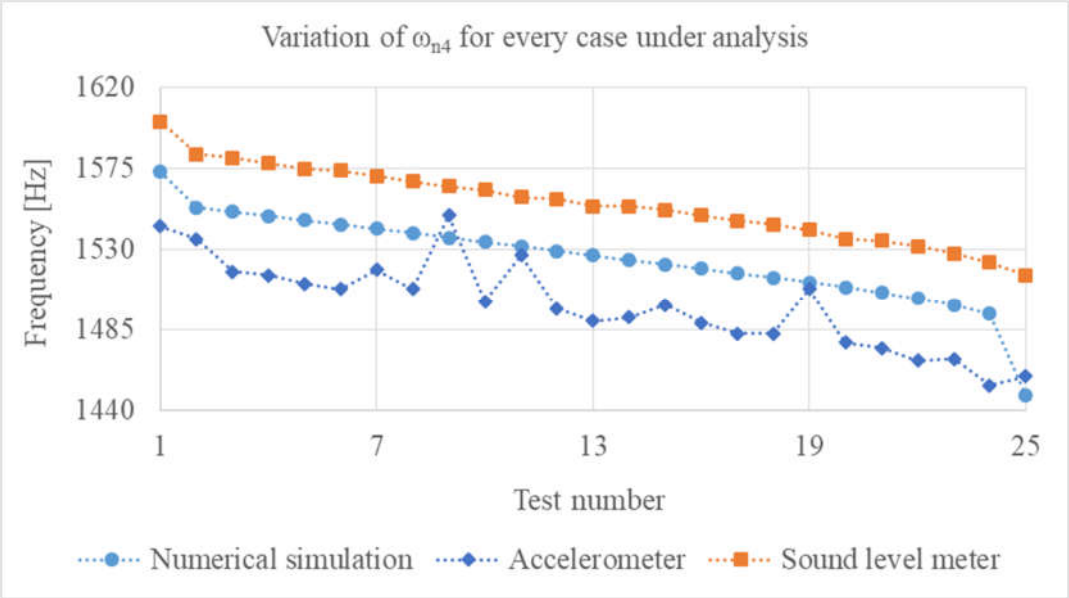

Figure 25. Global analysis of the fourth natural frequency variation along the tests.

4.8. Damping ratios

Figure 26 shows the variation of the damping ratio along all the tests performed on the beams.

It is possible to notice that the damping ratio associated with the first vibration mode increases along the tests despite its oscillation on some tests. The damping ratio associated with the second vibration mode is not significantly affected and it also oscillates on some tests. The damping ratio associated with the third vibration mode oscillates a significantly along almost every test (it will be discussed on next chapter).

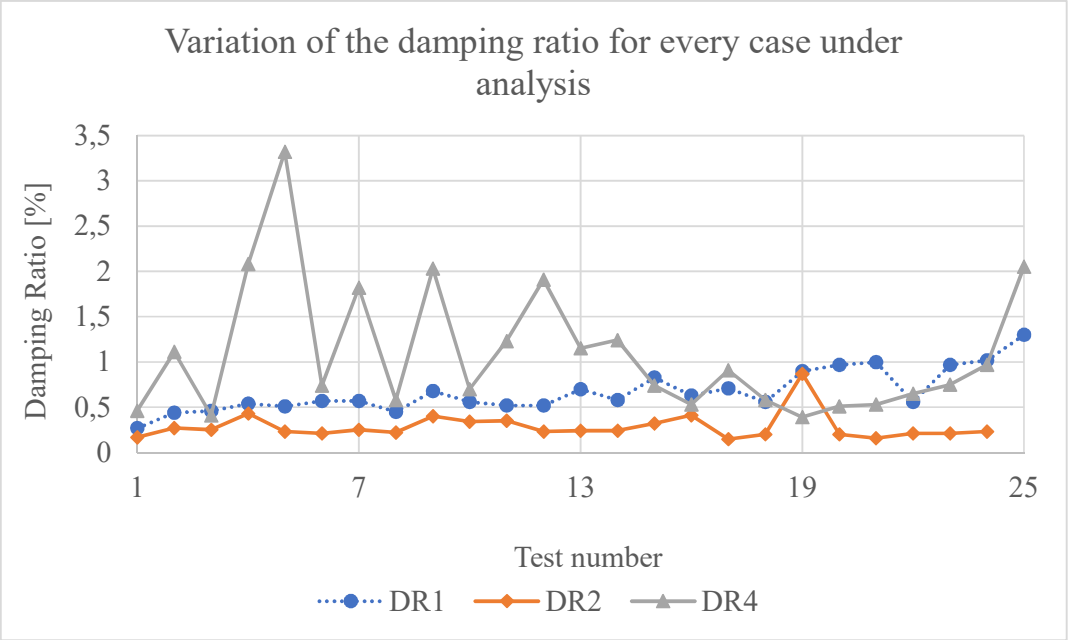

Figure 26. Damping ratios measured along the tests.

4.9. FRF analysis

The impact tests allows us to analyze the FRFs' behavior along the tests. It is an interesting approach that allows noticing how the amplitude of the response varies along the tests and which mode is predominating on the dynamic behavior.

Figure 27 shows the FRF behavior along the tests. Many tests were performed and would be nearly impossible to analyze the data if they were plotted all on the same graph, so, some tests were chosen to represent the modal behavior ($T_{1,1}$, $T_{3,2}$ and $T_{4,7}$). These tests were chosen because they represent: the undamaged beam ($T_{1,1}$); the beam with a medium severity level ($T_{3,2}$); and the most damaged beam ($T_{4,7}$).

It is possible noticing that the measured natural frequency decreases its value, according with the expected, because the tests performed on the beams with greater damage severity levels have their peaks dislocated to the left. Moreover, it is possible to notice that the first and third natural frequencies are the most affected on their values, while the frequency associated with the second mode shape is not affected as much as the previous ones.

Analyzing the amplitude variation, it is noticeable that the one associated with the third peak (fourth mode for $T_{1,1}$ and $T_{3,2}$ and fifth mode for $T_{4,7}$) is the most affected

along the tests (the last value decreases approximately 75 % when compared with the first one). Followed by the first mode, which also have the amplitude affected but not as much as the previous one. Again, the second natural frequency is not significantly affected.

Another aspect to be observes is that the amplitude variation of the third natural frequency is bigger between $T_{1,1}$ and $T_{3,2}$ than between $T_{3,2}$ and $T_{4,7}$. While for the first natural frequency, the greater variation occurs between $T_{3,2}$ and $T_{4,7}$.

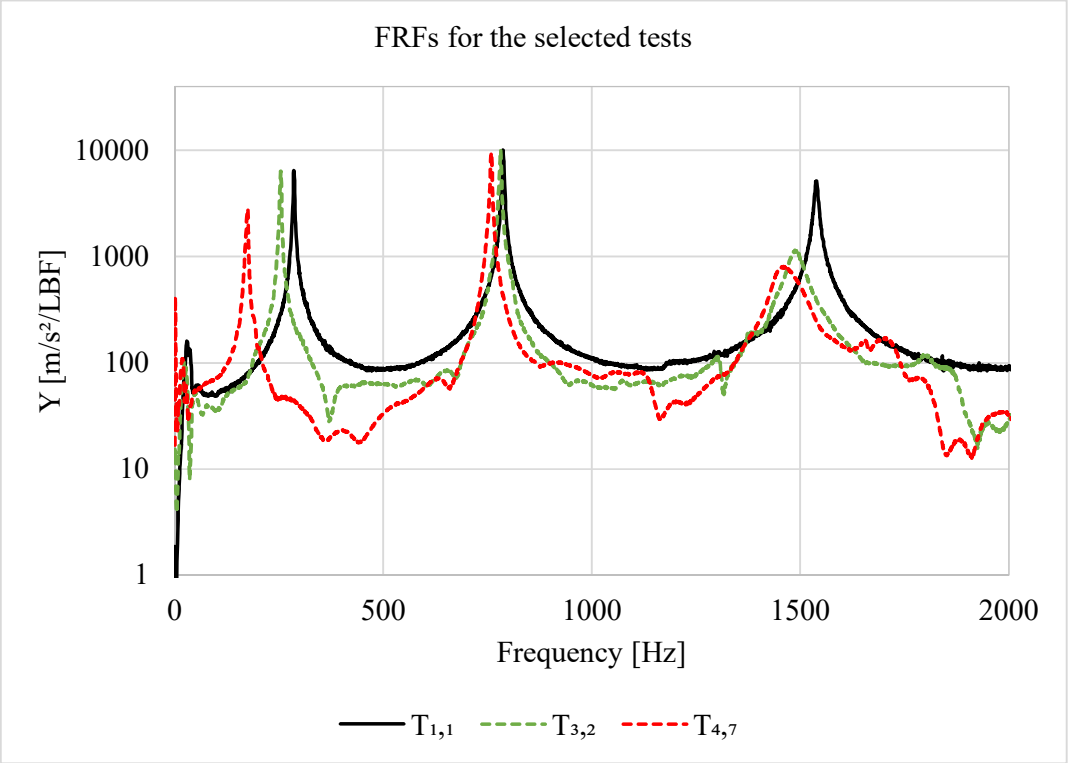

Figure 27. FRFs for the selected tests performed.

5. DISCUSSION

In this section, the results will be discussed and the correlated with the theory. Yet, this is an essential part to understand and evaluate the conclusions (Chapter 6).

5.1. Natural frequencies

On this section, the damage effects on the natural frequencies and damping ratios and the errors between the estimated and measured values obtained during the numerical simulation and the tests performed will be discussed.

5.1.1. Damage effects

It is possible to observe a decrease on the values of all the natural frequencies on the range under analysis. In addition, most of these frequencies are related the flexural modes of vibration (there are three flexural modes and one torsional mode of vibration). The damage inflicted causes a significant reduction on the moment of inertia of the beam (37,50% for the first diameter and almost 95% for the last one – considering the center of the beam), causing a decrease of the beam's bending stiffness, consequently, decreasing the value of the natural frequencies associated with these vibration modes.

It is noticeable that the decrease on the natural frequency value is higher on the frequency of the first bending (or flexural) vibration mode. This mode's frequency decreases by, approximately, 39,20% when compared with the value obtained in the undamaged condition. In sequence, the natural frequency of the third bending (or flexural) mode is the most affected (considering only bending modes), it decreases, approximately, 5,44%. Notice how, for both modes, the point most affected by the damage infliction is a point of maximum displacement value (absolute for the first bending mode and local for the third mode). When damaged, the point of maximum displacement requires less energy to strain (the bending stiffness decreases), justifying the higher decrease of the first bending mode when compared with the decrease measured for the third bending mode (the third bending mode has only one of its three maximum points affected by the damage).

The second bending mode is not as much affected as the first bending mode (decreases approximately 3,60%). One possible reason is that the damage is located

around a nodal line (the point that acts like a rotation point to allow the bending), so the damage changes the bending stiffness and the inertia moment, but the result is not so significant. The small variation can be associated with the damage infliction method: perforations were performed, implying that not only the line was affected but, also, the circle area around the central point of the beam, decreasing the stiffness and the energy required to strain the adjacent points and reducing the energy level required to vibrating on this mode.

The third natural frequency, corresponding to the first torsional mode, also shows a considerable decrease on its value (decreases approximately 26,70%). Again, the damage is responsible for the decrease. The decrease on the beam's inertia moment also reduces the polar moment of inertia, reducing the torsional stiffness, affecting the natural frequency (similarly to the bending modes).

Some natural frequencies increased during the tests performed (see details on each beam's result item). This was not expected and, probably is related with the inability of the operator who performed the tests. Double impact or accelerometer not fixed hard enough are some possible reasons to obtain this erroneous data. In addition, the fourth mode (third bending mode) was the most affected. This mode, particularly, had its amplitude hugely affected by the damage inflicted and, on some tests, there was not a well defined peak on its natural frequency region.

5.1.2. Tests using accelerometer and the sound level meter

The results obtained using the accelerometer and the sound level meter to measure the output data obtained similar results. Considering all the tests for all the beams, the average error between the values measured with the accelerometer and the values measured with sound level meter is 4,01%, the maximum error is 5,23% and the standard deviation is 0,57%. For the data obtained simultaneously using the accelerometer and the sound level meter the average error is 0,22%, the maximum error is 2,18% and the standard deviation is 0,37%. This difference can be due to the mass loading caused by the accelerometer (causes a decrease on the natural frequencies) or the damping of air. Additionally, the accelerometer cable can influence the damping, once it absorbs a part of the kinetic energy of the beam.

The error between the results estimated during the numerical simulation and the measured with the sound level meter are small as well. The average error is 2,07%, the maximum error is 4,74% and the standard deviation is 0,80%.

For comparison, the error between the values estimated during the numerical simulation and the measured using the accelerometer to measure the output data has a medium value of 1,67%, a maximum value of 2,68% and a standard deviation of 0,54%.

The measurements using the sound level meter to measure the output data obtained higher natural frequency values for all the bending modes, when compared both with the measured values using the accelerometer and the estimated values obtained during the numerical simulation. This can be due to the mass loading caused by the accelerometer, which influences, mostly, the bending modes. For the torsional mode the sound level meter obtained a lower value for the natural frequency, except for $T_{4,6}$.

Another point to consider is that the tests performed using both methods to measure the output data (using the accelerometer and the sound level meter) simultaneously does not allow to measure the natural frequency associated with the torsional mode. It can be due damping addition caused by the accelerometer cable.

5.2. Mode shapes

As seen in chapter 4, the mode shapes on the range under analysis does not change for the beam one, two and three. The beam number four has its fourth vibration mode changed on the last set of tests (the third bending mode turns the fifth mode acting on the beam).

The damage inflicted, apparently, is not enough severe to change the vibration modes until the last diameter tested on the beam.

One thing to consider is that the damage location is always the same (varying only its diameter). The mode shapes may be most affected by the localization of the damage than its severity.

Unfortunately, the mode shapes were only obtained during the numerical simulations, due to the lack of software to do so.

5.3. Damping ratios

The damping ratios were calculated using the half bandwidth method, for each natural frequency on the range under analysis.

It is possible to observe an increase on the damping ratio associated with the first vibration mode. However, it is not enough to conclude it happens because of the damage inflicted (the variation is not considerable).

The damping ratio associated with the second vibration mode oscillate on some tests but does not change considerably along the tests. Apparently, the damage infliction does not change this property.

The damping ratios associated with the fourth vibration mode (third natural frequency measured on the FRFs) oscillates along all the tests but the values obtained for the last set of tests indicate an increase on its value. This mode, specifically, is the most affected (when talking about the vibration amplitude) along the tests. Looking the FRFs variation (section 4.9) gives a better perspective of this behavior.

5.4. Frequency response functions

The analysis of the obtained FRFs shows the behavior along the performed tests. It is noticeable the decrease on the value of the first and third natural frequencies. Though, in percentage level, the variation on the value of the third natural frequency is not as much bigger as the first one, the absolute variation is still considerable (the percentage variation is, approximately, 5,44% but the value variation is, approximately, 84Hz vs 111Hz for the first natural frequency). In addition, it is possible to observe that the second bending has no much effect on its natural frequency or on its peak amplitude, showing that the damage does not affect this mode with the same severity it affects the others.

The peak amplitude of the third natural frequency (third bending mode) is the most affected. The values obtained for the last test performed decreases, approximately, 75,30% from the value obtained during the tests on the undamaged beam, becoming nearly totally damped. The second most affected mode is the first bending mode decreasing approximately 33,20% when compared with the measurements during the first test performed. The variation for the second bending mode is around 12,10%.

Furthermore, it is possible to visualize that the damage severity affects mostly the third bending mode until, approximately, the half of the damage severity. After that, the effect is bigger on the first bending mode.

6. CONCLUSIONS AND FUTURE RESEARCH SUGGESTIONS

The numerical procedure provided enough values to use as reference for the values obtained during the experimental procedure. Moreover, the experimental procedures provided enough data to analyze end compare the values obtained for the natural frequencies and damping ratios using both measurement methods. Analyzing and comparing the obtained data allows reaching the following conclusions.

6.1. Conclusions

First, the measurements performed using the sound level meter to measure the output data are reliable. As discussed before, the values estimated during the numerical simulations and measured using the accelerometer and the sound level meter were close enough to consider its usage when the accelerometer usage is not possible. However, some conditions need to be satisfied to use the sound level meter to measure the natural frequencies and the damping ratio for a system, mainly:

1. The system under analysis cannot be heavily damped because the vibration is quickly damped, implying the system stops vibrating before the measurement is concluded or the signal has not enough energy to be measured.
2. The measurements need to be done, preferably, on an ambient with no background noise or with a low-level background noise. The measurements can be interfered for the noise, generating uncertainties on the measurements.
3. The measurement time must be chosen according to the time the system is under vibration; otherwise, the data obtained can represent only a part of the vibration or be contaminated with background noise.

The second conclusion is that the damage inflicted on the beam affects, directly, the natural frequencies and their values decrease along the experiments due to the reduction on the stiffness of the beam. All the frequency values measured during the experimental procedures decreased but the magnitude of the decrease depends on the vibration mode. For this beam, the first bending mode was the most affected by the natural frequency value decrease (considering the percentage variation from the first to

the least measured value), followed by the first torsional mode, the third bending mode and, last, the second bending mode.

The third conclusion is that the locations for the input and measurement of the output signals (when using the accelerometer to measure the output data) must be chosen according to the mode shapes required for analysis. For example, during the experiments performed, the third natural frequency (torsional mode) could not be measured using the accelerometer due to the bad position of the excitation and measurement points chosen for this case. When using the sound level meter to measure the output data, the torsional mode will still contribute for the acoustical response, even if the measurement is performed on the neutral line of the beam.

The damping ratios associated with the first and fourth vibration modes increases along the tests. The increase on its value can be associated with an increase of internal friction due to the decrease on the stiffness of the beam, caused by the damage inflicted. However it is not possible to conclude that the this variation was due to the damage inflicted.

6.2. Future research suggestions

Even with the amount of data collected and analyzed on this work, there are still some unanswered questions. It leads us to suggest some topics for future researches:

1. Study of multiple damages or single damage with different locations, aiming to study its impacts on the modal parameters, mainly the mode shapes.
2. Measure the vibration response using the sound level meter at different distances from the beam, aiming to verify the distance's impact on the obtained data (its quality and if there is the need to consider some damping of the medium when a certain distance is reached).
3. Measure the vibration response using multiple sound level meters, aiming to obtain the modal parameters for the system; specifically the mode shapes (by triangulation or other method to locate the source of the acoustic response).
4. Measure the vibration response in more than one direction aiming to observe the change on the modal behavior, specifically the mode shapes.

LIST OF REFERENCES

[1] S. S. Rao, *Mechanical Vibrations*, 5th ed., vol. 67. Upper Saddle River: Pearson, 2010.

[2] H. F. G. Genari, "Métrica Baseada em Projeção de Modelos para Detecção de Danos em Estruturas," Universidade Estadual de Campinas, 2012.

[3] A. Güemes, *Structural HealthMonitoring*, 1st ed. London: ISTE Ltd, 2006.

[4] J. Humar, A. Bagchi, and H. Xu, "Performance of vibration-based techniques for the identification of structural damage.pdf," *Struct. Heal. Monit.*, vol. 5, no. 3, p. 27, 2006.

[5] E. P. Carden and P. Fanning, "Vibration Based Condition Monitoring: A Review," *Struct. Heal. Monit.*, vol. 3, no. 4, pp. 355–377, 2004.

[6] R. J. Allemang and W. R. Shapton, "Using Modal Techniques to Guide Acoustic Signature Analysis," in *SAE 780106*, 1979, pp. 385–393.

[7] W. Elwali, H. Satakopan, V. Shauche, R. Allemang, and A. Phillips, "Modal Parameter Estimation Using Acoustic Modal Analysis," in *Proceedings of the IMAC-XXVIII*, 2010, vol. 3, pp. 23–33.

[8] D. J. Inman, *Engineering Vibration*, 4th ed. New Jersey: Pearson Education, 2013.

[9] D. J. Ewins, *Modal Testing*, 2nd ed. Philadelphia: Research Studies Press Ltd, 2000.

[10] C. C. Kennedy and C. D. P. Pancu, "Use of Vectors in Vibration Measurement and Analysis," *J. Aeronaut. Sci.*, vol. 14, No 11, pp. 603–625, 1947.

[11] N. M. M. Maia *et al.*, *Theoretical and Experimental Modal Analysis*. Philadelphia: Research Studies Press Ltd, 1998.

[12] R. J. Allemang, "Experimental modal analysis. [for vibrating structures]," Cincinnati.

[13] B. J. Schwarz and M. H. Richardson, "By," pp. 1–12, 1999.

[14] P. Avitabile, "Is there any real advantage to MIMO testing?," *SEM Exp. Tech.*, pp. 1–2.

[15] M. A. Peres, C. Kallmeyer, M. C. Witter, R. Carneiro, F. D. Marques, and L. P. R. De Oliveira, "Advantages of Multiple-Input Multiple-Output (MIMO) testing using low level excitation systems," pp. 1121–1134.

[16] M. Batel, "Operational Modal Analysis – Another Way of Doing Modal

Testing," 2002.

[17] M. H. Richardson and V. Technology, "Is It a Mode Shape or an Operating Deflection Shape?," 1997.

[18] B. J. Schwarz and M. H. Richardson, "INTRODUCTION TO OPERATING DEFLECTION SHAPES," pp. 1–7, 1999.

[19] J. C. Maxwell, "Scientific Papers," vol. 1, p. 598, 1890.

[20] F. Fahy, *Foundations Of Engineering Acoustics*. Southampton: Academic Press, 2000.

[21] L. E. Kinsler and A. R. Frey, *Fundamentals of Acoustics*, 2nd ed. New York and London: John Willey and Sons, Inc., 1962.

[22] M. F. Jardim, "Análise Teórica e Experimental Vibro-Acústica Utilizando a Técnica de Matrizes Compactas," UNESP, 2008.

[23] M. Vivolo, "Vibro-acoustic Characterization of Lightweight Panels by using a Small Cabin," KU Leuven, Heverlee, 2013.

[24] L. C. da S. M. Cardoso, "Interacção Vibroacústica do Sistema Placa-Cavidade Fechada:," Universidade do Porto, 2010.

[25] L. F. Vales, "Análise numérica da influência de parâmetros estruturais no desempenho vibriacústico de placas flexíveis," Universidade de São Paulo, 2018.

[26] E. V. G. Silva, "Determinação do amortecimento de materiais por meio da técnica de excitação por impulso," Pato Branco, 2015.

[27] L. Meirovitch, *Principles and techniques of vibrations*. 1997.

[28] A. K. Pandey and M. Biswas, "Damage Detection in Structures Using Changes in Flexibility," *J. Sound Vib.*, vol. 169(1), pp. 3–17, 1994.

[29] D. Bernal, "Damage Localization using Load Vectors," in *Europ. COST Conf. On System Indentification & Structural Health Monitoring*, 2000, pp. 223–232.

[30] D. Bernal, "Load Vectors for Damage Localization," *J. Eng. Mech.*, vol. 128(1), pp. 7–14, 2002.

[31] N. Stubbs, J. Kim, and C. Farrar, "Field Verification of a Nondestructive Damage Localization and Severity Estimation Algorithm," *Int. Modal Anal. Conf. 13*, pp. 210–218, 1995.

[32] K. WORDEN, G. MANSON, and D. J. ALLMAN, "An Experimental Appraisal of the Strain Energy Damage Location Method," in *Proc. 4th Intl. Conference on Damage Assessment of Structures (DAMAS 2001)*, 2001, pp. 35–46.

[33] J. Maeck, "Damage Assessment of Civil Engineering Structures by Vibration

Monitoring," KU Leuven, 2003.

[34] H. Sohn, C. R. Farrar, F. Hemez, and J. Czarnecki, "A Review of Structural Health Monitoring Literature 1996 – 2001," *Third World Conf. Struct. Control*, no. DECEMBER, pp. 1–7, 2002.

APPENDIX A

Table 9. Properties of the beams.

Property	Value	Unit
E	70	Gpa
ρ	2710	kg/m³
m_{approx}	0,1626	kg
$I_{undamaged}$	4,1667	$x10^{-10}$ m^4
L (bar length)	300	mm

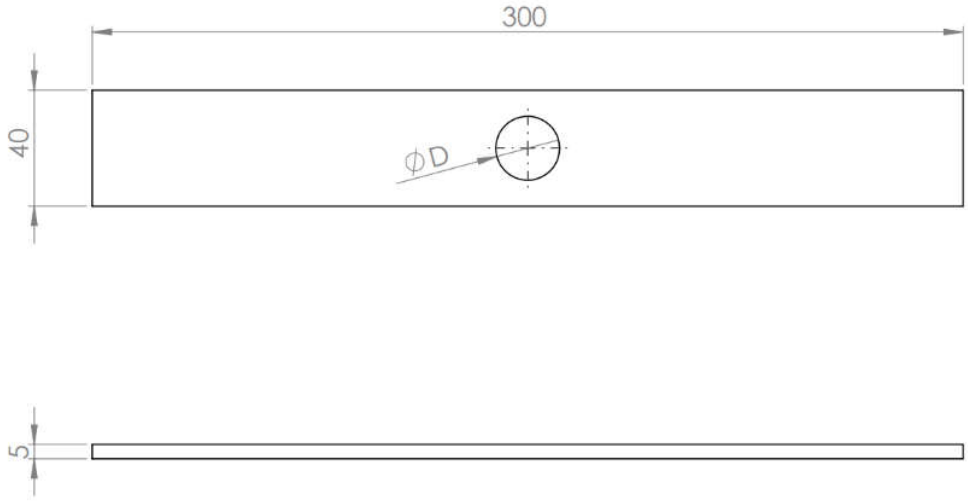

Figure 28. Schematic of the damaged beam. Dimensions in mm.

It is worth remembering that the dimension "D" in Figure 28 can assume any integer value between 15 and 38 mm.

APPENDIX B

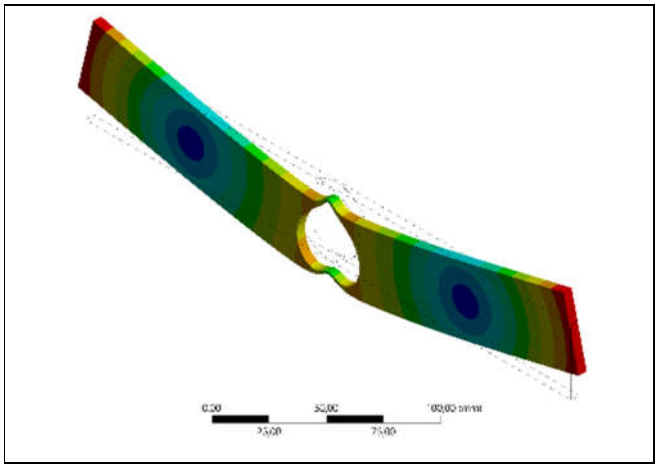

Figure 29. Sixth mode shape for $T_{4,7}$ (1650,7 Hz).

Table 10. Errors between the estimated and measured (using accelerometer) natural frequencies.

		T_1	T_2	T_3	T_4	T_5	T_6	T_7
Beam 1	ω_{n1}	1,991	1,519	1,732	2,158	1,649	1,774	1,636
	ω_{n2}	1,824	1,755	1,888	2,104	1,930	1,902	1,780
	ω_{n3}	NA	NA	NA	NA	NA	NA	NA
	ω_{n4}	1,926	1,114	2,134	2,118	2,296	2,338	1,472
		T1	T2	T3	T4	T5	T6	T7
Beam 2	ω_{n1}	1,991	1,402	1,364	1,926	1,302	1,489	1,586
	ω_{n2}	1,824	1,667	2,009	2,045	1,985	1,918	1,751
	ω_{n3}	NA	NA	NA	NA	NA	NA	NA
	ω_{n4}	1,989	2,027	0,794	2,170	0,313	2,118	2,417
		T1	T2	T3	T4	T5	T6	T7
Beam 3	ω_{n1}	1,785	1,346	0,735	1,441	0,735	0,663	0,915
	ω_{n2}	1,749	1,823	1,405	1,750	1,776	1,766	1,503
	ω_{n3}	NA	NA	NA	NA	NA	NA	NA
	ω_{n4}	1,989	2,125	1,511	2,007	2,241	2,080	0,258
		T1	T2	T3	T4	T5	T6	T7
Beam 4	ω_{n1}	1,991	0,722	0,885	1,308	0,343	0,262	0,433
	ω_{n2}	1,824	1,763	1,896	2,221	1,839	1,830	1,828
	ω_{n3}	NA	NA	NA	NA	NA	NA	NA
	ω_{n4}	2,117	2,061	2,071	2,322	2,001	2,677	0,739
		Average error						1,665
		Maximum error						2,677
		Standard deviation						0,537

Table 11. Errors between the estimated and measured (using the sound level meter and accelerometer) natural frequencies.

		T1	T2	T3	T4	T5	T6	T7
Beam 1	ω_{n1}	NA	1,510	1,750	1,953	1,667	1,783	1,399
	ω_{n2}	NA	1,521	1,847	2,341	1,927	1,977	1,786
	ω_{n3}	NA	NA	NA	NA	NA	NA	NA
	ω_{n4}	NA	2,723	2,069	2,311	0,162	2,208	1,732
		T1	T2	T3	T4	T5	T6	T7
Beam 2	ω_{n1}	NA	1,640	0,857	1,944	1,292	1,489	1,356
	ω_{n2}	NA	1,748	1,234	2,042	1,904	1,993	1,679
	ω_{n3}	NA	NA	NA	NA	NA	NA	NA
	ω_{n4}	NA	2,482	1,379	2,236	0,796	2,184	2,351
		T1	T2	T3	T4	T5	T6	T7
Beam 3	ω_{n1}	NA	1,355	0,735	1,202	0,999	1,098	1,201
	ω_{n2}	NA	1,901	1,484	1,757	1,776	1,851	1,980
	ω_{n3}	NA	NA	NA	NA	NA	NA	NA
	ω_{n4}	NA	1,929	1,445	1,941	2,241	2,146	0,390
		T1	T2	T3	T4	T5	T6	T7
Beam 4	ω_{n1}	NA	0,168	0,874	1,623	0,331	0,236	0,405
	ω_{n2}	NA	1,760	1,896	2,300	1,839	1,756	1,915
	ω_{n3}	NA	NA	NA	NA	NA	NA	NA
	ω_{n4}	NA	2,193	2,005	2,655	2,068	2,744	0,366
		Average error						1,637
		Maximum error						2,744
		Standard deviation						0,614

Table 12. Errors between the estimated and measured (using the sound level meter) natural frequencies.

		T1	T2	T3	T4	T5	T6	T7
Beam 1	ω_{n1}	2,522	2,695	2,696	2,961	2,599	2,733	2,917
	ω_{n2}	1,916	1,987	2,005	1,949	1,896	2,004	1,961
	ω_{n3}	1,608	1,485	1,449	1,472	1,453	1,401	1,392
	ω_{n4}	1,761	1,912	1,928	1,885	1,843	1,936	1,900
		T1	T2	T3	T4	T5	T6	T7
Beam 2	ω_{n1}	2,522	2,707	2,784	2,935	2,693	3,010	2,714
	ω_{n2}	1,838	2,048	1,970	1,945	1,851	1,843	1,925
	ω_{n3}	1,688	1,340	1,417	1,263	1,394	1,379	1,294
	ω_{n4}	1,697	1,871	1,835	1,871	1,776	1,870	1,775
		T1	T2	T3	T4	T5	T6	T7
Beam 3	ω_{n1}	2,522	2,765	3,196	3,040	3,316	3,045	3,301
	ω_{n2}	1,916	2,019	2,049	2,016	2,002	2,012	2,049
	ω_{n3}	1,608	1,120	1,034	1,019	1,890	0,871	0,809
	ω_{n4}	1,824	1,942	1,971	1,941	1,912	1,948	1,925
		T1	T2	T3	T4	T5	T6	T7
Beam 4	ω_{n1}	2,522	3,369	3,619	3,631	3,962	4,494	4,739
	ω_{n2}	1,916	1,802	1,993	2,000	1,998	2,019	1,966
	ω_{n3}	1,608	0,825	0,536	0,509	0,436	2,941	0,092
	ω_{n4}	1,761	1,783	1,912	1,936	1,935	1,941	4,674
		Average error						2,067
		Maximum error						4,739
		Standard deviation						0,799

Table 13. Errors between the measured natural frequencies (accelerometer and sound level meter).

		T1	T2	T3	T4	T5	T6	T7
Beam 1	ω_{n1}	4,605	4,279	4,506	5,232	4,319	4,588	4,629
	ω_{n2}	3,810	3,810	3,968	4,140	3,901	3,981	3,809
	ω_{n3}	NA	NA	NA	NA	NA	NA	NA
	ω_{n4}	3,759	3,060	4,150	4,090	4,236	4,377	3,423
		T1	T2	T3	T4	T5	T6	T7
Beam 2	ω_{n1}	4,605	4,167	4,206	4,956	4,048	4,567	4,369
	ω_{n2}	3,730	3,777	4,060	4,074	3,914	3,834	3,741
	ω_{n3}	NA	NA	NA	NA	NA	NA	NA
	ω_{n4}	3,761	3,979	1,033	4,131	2,096	4,075	4,295
		T1	T2	T3	T4	T5	T6	T7
Beam 3	ω_{n1}	4,386	4,167	3,960	4,546	4,081	3,732	4,256
	ω_{n2}	3,730	3,914	3,503	3,833	3,846	3,846	3,605
	ω_{n3}	NA	NA	NA	NA	NA	NA	NA
	ω_{n4}	3,891	4,155	3,536	4,030	4,248	4,113	2,188
		T1	T2	T3	T4	T5	T6	T7
Beam 4	ω_{n1}	4,605	4,121	4,544	5,005	4,321	4,221	4,287
	ω_{n2}	3,810	3,629	3,964	4,316	3,909	3,921	3,865
	ω_{n3}	NA	NA	NA	NA	NA	NA	NA
	ω_{n4}	3,961	3,924	4,068	4,360	4,016	4,746	3,907
		Average error						4,014
		Maximum error						5,232
		Standard deviation						0,567

Table 14. Errors between the measured natural frequencies (accelerometer and sound level meter with the accelerometer).

		T1	T2	T3	T4	T5	T6	T7
Beam 1	ω_{n1}	NA	0,009	0,018	0,210	0,018	0,009	0,240
	ω_{n2}	NA	0,238	0,041	0,242	0,003	0,076	0,006
	ω_{n3}	NA	NA	NA	NA	NA	NA	NA
	ω_{n4}	NA	1,628	0,066	0,198	2,184	0,133	0,263
		T1	T2	T3	T4	T5	T6	T7
Beam 2	ω_{n1}	NA	0,241	0,514	0,019	0,010	0,000	0,234
	ω_{n2}	NA	0,083	0,791	0,003	0,083	0,077	0,073
	ω_{n3}	NA	NA	NA	NA	NA	NA	NA
	ω_{n4}	NA	0,464	0,581	0,067	1,113	0,067	0,067
		T1	T2	T3	T4	T5	T6	T7
Beam 3	ω_{n1}	NA	0,010	0,000	0,243	0,266	0,438	0,289
	ω_{n2}	NA	0,080	0,080	0,006	0,000	0,087	0,484
	ω_{n3}	NA	NA	NA	NA	NA	NA	NA
	ω_{n4}	NA	0,201	0,067	0,067	0,000	0,067	0,133
		T1	T2	T3	T4	T5	T6	T7
Beam 4	ω_{n1}	NA	0,559	0,011	0,319	0,012	0,026	0,029
	ω_{n2}	NA	0,003	0,000	0,081	0,000	0,075	0,089
	ω_{n3}	NA	NA	NA	NA	NA	NA	NA
	ω_{n4}	NA	0,135	0,068	0,341	0,068	0,069	1,097
		Average error						0,216
		Maximum error						2,184
		Standard deviation						0,368